RECOVERY BEHAVIOR OF SHAPE MEMORY POLYMER BASED LAMINATES

RECOVERY BEHAVIOR OF THERMOPLASTIC SHAPE MEMORY POLYURETHANE BASED LAMINATES AFTER THERMOFORMING- VARIED MODULUS OF POLYURETHANES

By SHUILIANG WU, B. Eng, M. Sci.

A Thesis Submitted to the School of Graduate Studies in Partial Fulfillment of the Requirements for the Degree Master of Applied Science

MASTER OF APPLIED SCIENCE (2015) McMaster University

(Chemical Engineering) Hamilton, Ontario

TITLE: Recovery Behavior of Thermoplastic Shape Memory polyurethane Based Laminates after Thermoforming- Varied Modulus of Polyurethanes

AUTHOR: Shuiliang Wu

B. Eng. (Nanjing University of Science & Technology, China)

M. Sci. (Zhejiang University, China)

SUPERVISOR: Dr. Michael R. Thompson

NUMBER OF PAGES: xix, 91

Lay Abstract

Special classes of Polyurethanes exhibit a strong memory of their formed shape, and hence are called shape memory polymers. Films made of these polymers are envisioned as a replacement for decorative applications in automobiles if their forming behaviour is understood. This thesis project looked at how much of that memory was preserved as a laminate after thermoforming by looking at the effect of film stiffness, backing material used (polypropylene (PP) versus acrylonitrile butadiene styrene (ABS)), ambient temperature and the extent of deep draw, using both experimental and modelling methods. Results showed that through using stiffer films, weaker substrates, high ambient temperature or an optimal extent of deep draw, recovery behavior of the shape memory polymer in these laminates can be improved, and vice versa.

Abstract

In recent decades, a type of shape memory polymers (SMPs), namely thermoplastic shape memory polyurethane (shape memory TPU, using TPU for short) has drawn considerable attention for its excellent shape memory properties, versatile structure and good mechanical properties. Most recently, shape memory TPU films are envisioned as a replacement for automobile exterior and interior decorative applications in the forms of laminates through in-mold forming (IMF) process. However, for a better dimensional control of laminates during the IMF, the shape memory effect of laminates needs to be controlled such that its behaviour is only noted at the time of damage and is not an instigator of delamination.

In order to investigate the shape memory behavior of TPU based laminates after they had experienced normal processing such as by thermoforming, the influence of different properties were examined, including TPU film modulus, substrate used (polypropylene (PP) versus acrylonitrile butadiene styrene (ABS)), ambient temperature and the extent of deep draw, on the recovery behaviour. The study included analyses through both experimental and modelling methods.

A novel thermo-mechanical cycling method was proposed to examine the shape memory property of the TPU based laminates under stretching/bending conditions more similar to thermoforming. Recovery based on this method was defined using new terms of angle recovery ratio and recovery rate. The new test examined recovery at 15^{o}C, 45^{o}C and 65^{o}C; these ambient conditions were selected above and below the glass transition temperature of the TPU. Results showed that the final angle recovery ratio and recovery

rate of deformed laminates based on a new commercial class of TPU shape memory polymer increased with its modulus from low to high. Substrates of higher modulus (ABS) lowered the final angle recovery ratio and recovery rate achievable for a formed laminate. Furthermore, increasing the ambient temperature increased both the final angle recovery ratios and recovery rates of formed TPU based laminates. As the extent of draw changed from 6 mm to 10mm, the final angle recovery ratios and recovery rates of formed laminates increased for all TPU films but this trend was reversed when the draw further increased beyond 10mm.

The laminate system was subsequently modelled using a linear viscoelastic (SLV) constitutive model to analyze the stress-strain relationship between the substrate and TPU film layers during recovery. A model parameter related to stress transfer across the interface of these two polymer layers was fitted to the experimental results with an excellent degree of fit. The model results fitted well with experimental data and showed that the final angle recovery ratios of formed TPU laminates were mainly dependant on the moduli of TPU and substrates layers as well as the stress transfer ratio through the adhesive layer (*TR*). The influence of the adhesive layer was not a trivial variable in the recovery nature of the laminate. The influence of ambient temperature on the recovery behaviour of laminates was mainly due to the temperature-dependent and time-dependent Young's modulus and relaxation time of both TPU and substrate layers. Higher relaxation times for the TPU layer or lower relaxation time for the substrate layer yielded a higher recovery rate for the laminate during the first five minutes of recovery.

Acknowledgements

Upon the completion of this dissertation, I want to first express my deepest gratitude to my supervisor, Dr. Michael R. Thompson, for giving me the opportunity to work on this project and continuing guidance and innovative supports over past two years to my dissertation research. Besides, I had the opportunity to work in other project under his supervision and his invaluable scientific knowledge and expertise on extrusion helped me develop the cross-disciplinary knowledge. I also had the opportunity to be selected as a teaching assistant for his undergraduate lab course for which I am very grateful. I will be always appreciated for his considerate arrangements on me during these two years, which is very helpful to me.

I would like to extend my gratefulness to Kent Nielsen for his technical advice and timely supply of materials to the research. I appreciate the financial support extended from NSERC, 3M Canada and McMaster University for the duration of this work. Also, I want to thank Dr. Mukesh K. Jain for his suggestions during the company meeting.

It is my pleasure to have my project member and friend, Wensen Xu, in past two years. A lot of ideas came from the discussion between us even in the personal time. His mechanical engineering background brought several perspectives that were fresh to me. He also provided good suggestions to my modeling work in this thesis. Special thanks to Dr. Prasath Balamurugan for leading me into this project quickly and many suggestions at the beginning of the work.

A number of people have given me help during the dissertation research. I would like to appreciate the training, guidance and support from Ms. Elizabeth Takacs. Very

special thanks go to Paul Gatt and Dan Wright for their continual technical supports for my experiments, without which the work can never be implemented. Also I want to give thanks to Ms. Kathy Goodram, Ms. Lynn Falkiner, Ms. Cathie Roberts for their administrative assistance.

It has been my great honor to study and work with so many lovely people: Huiying Li, Yang Liu, Ali Goger, Zeinab Mousavi Khalkhali, Qiang Fu, Xudong Deng, Zhuyuan Zhang and other friends and group members for their friendship and supports.

Last but most important, I want to thank my parents and parents-in-low for being supportive for my graduate study and new life in Canada, and my wife, Hongxia Chen and my lovely son, Roger Shuhao Wu, for their love that is beyond the expression of any words.

Table of Contents

List of Figures and Tables

List of All Abbreviations and Symbols

SMPs	Shape memory polymers
PUs	Polyurethanes
TPU	Thermoplastic shape memory polyurethane
PP	Polypropylene
ABS	Acrylonitrile butadiene styrene
TT	3M adhesive transfer tape 468MP
IMF	In-mold forming
IMD	In-mold decorating
IML	In-mold labelling
VOCs	Volatile organic compounds
SLV	Standard linear viscoelastic
ASTM	American standard test method
MR	Isocyanate-polyol ratios
DSC	Differential scanning calorimetry
DMA	Dynamic mechanical analysis
UMTS	Universal mechanical testing system
DV	Draw values
t	Time, [units of s]
T	Temperature, [units of ^{o}C]
TR	Stress transfer ratio through the adhesive layer, [units of %]

T_{trans}	Transition temperature, [units of ^{o}C]
T_m	Melting temperature, [units of ^{o}C]
T_g	Glass transition temperature, [units of ^{o}C]
R_r	Strain recovery rate, [units of %]
R_f	Strain fixity rate, [units of %]
ε	Strain, [units of %]
σ	Stress, [units of N/m^2]
E	Modulus, [units of MPa]
η	Viscosity, [units of Pa s]
$R_a(t)$	Angle recovery ratio, [units of %]
$R_{a,\,final}$, %	Final angle recovery ratio after 24h, [units of %]
$\alpha(0)$	Initial central angle after forming, [units of ^{o}]
$\alpha(t)$	Central angle of formed laminate at time t, [units of ^{o}]
E_{1a}	Relaxation modulus, [units of MPa]
E_{1b}	Non-equilibrium modulus, [units of MPa]
τ	Relaxation time, [units of s]
G'	Storage modulus, [units of MPa]
G"	Loss modulus, [units of MPa]
d	Original value of width or thickness of layers, [units of m]
Δd	Change of the width or thickness, [units of m]
ν	Poisson's ratio

L_0	Original length of laminate before forming, [units of m]
ΔL	Change of length of laminate after forming, [units of m]
$F(\theta, t)$	Recovery force from the TPU layer, [units of N]
A_T	Area of the cross-section of TPU layer after forming, [units of m^2]
A_S	Area of the cross-section of substrate layer after forming, [units of m^2]
$M_T(\theta, t)$)	Restorative bending moment at central angle of θ and time t, [units of N·m]
$M_T(t)$)	Overall restorative bending moment at time t, [units of N·m]
$M_S(t)$	Retarding bending moment at time t, [units of N·m]
$S(\theta, t)$	Arm of $F(\theta, t)$ at central angle of θ and time t, [units of m]
$r(t)$	Distance from the center of curvature O' to the centroid of the cross section of substrate layer at time t, [units of m]
$R(t)$	Radius of substrate layer at time t, [units of m]
H_S	Thickness of substrate layer after forming, [units of m]
L_S	Length neutral axis of substrate after forming, [units of m]
h	Draw value, [units of m]
R_m	Radius of the male mold, [units of m]
e	Distance between the neutral surface and centroid of a transverse section of the curved substrate layer at time t, [units of m]
T_{Recovery}	Recovery temperature, [units of ^oC]
k	Overall heat transfer coefficient of laminates, [units of K/s]
a, b, c, f and g	Constants representing slopes of straight lines on semi-logarithmic diagrams

Chapter 1 Introduction

1.1 Shape Memory Polymers (SMPs)

Generally, shape memory means the ability of a material to resume an original configuration after applied changes such as temperature or pressure. Among shape memory materials, shape memory polymers (SMPs) are a class of smart polymers capable of undergoing significant macroscopic deformation with the initiation of external stimuli, such as heat, electricity, magnetism, light and moisture (Behl and Lendlein, 2007, Behl et al., 2010, Leng and Du, 2012). Most recently, thermally responsive shape memory polymers have drawn greater attention from all over the world for their unique behaviour by being able to recover their original shape from heating, especially among the class of thermoplastic shape memory polyurethanes (TPUs) (Behl et al., 2010). The TPUs are segmented polyurethanes (PUs), a kind of (multi)block copolymer comprised of flexible soft segments and rigid hard segments, which are usually used as thermoplastic polyurethane elastomers in modern industries (Leng and Du, 2012). Because of their better versatility of chemical structure, lower cost, easier pre-treatment procedure, larger deformation and lower recovery temperature (Leng and Du, 2012), shape memory TPU are considered promising for a large variety of applications such as actuators (Koerner et al., 2004), biomedical materials (Meng et al., 2009), biodegradable sutures (Lendlein et al., 2001) and smart fibers (Zhu et al., 2006).

In the automotive industry, TPU films are developed in various manners based on their place of use in a vehicle and intended features. Due to their unrivaled scratch and mar resistance, shape memory TPU films have been used as a functional layer such as paint protection films to protect vulnerable areas like front bumpers, hoods, side mirrors,

door handle cavities, door edges, rocker panels, and rear fender panels from scratches, chips, stains and other damaging elements, keeping the vehicle looking newer longer.

1.2 In-Mold Forming Process

Thermoforming is a secondary forming technology for varieties of thermoplastic sheets or films (Throne, 2002). It needs pressure or vacuum to press or squeeze the hot thermoplastic sheets on the surface of molds to form a final shape. Thermoforming is considered as one of the most efficient processing methods due to its advantages like relatively short forming cycle, high forming speed, low cost for the molds, et al (Throne, 2002). It is suitable for automated production, especially with the continuous improvements made to thermoforming processes over time (Allard et al., 1986, Throne, 2008). A typical thermoforming process contains several steps including clamping, heating, shaping, cooling and trimming (Throne, 2008). With the development of those steps, thermoforming nowadays is much more complicated. Based on the number of steps in shaping, the methods of thermoforming can be divided into one-step thermoforming (vacuum forming, drape forming, free forming, pressure forming and matched mold forming), two-step thermoforming with pre-stretching (billow drape forming, vacuum snap-back forming, plug assisted vacuum/pressure forming), multi-step thermoforming (pressure bubble immersion forming) and other variations (Slip forming) (Throne, 2002, Throne, 2008).

As one of the most efficient and cost-effective ways of decorating a part, in-mold forming (IMF) is a processing technology to make compound components by firstly pre-forming an insert by thermoforming and then covering the insert with molten resin by injection molding, as shown in **Figure 1-1**. It is well known as in-mold decorating (IMD)

and in-mold labelling (IML) based on its different applications (Chen et al., 2010b). IMF offers many design and productivity advantages versus other methods done to cover a part after injection molding. These benefits include design flexibility, multiple colors and effects, textures with a single operation, long lasting graphics, manufacturing productivity, and system cost reductions (Chen et al., 2010b). It is suitable for small to medium-sized products, from automobile interior/exterior components with compound curves to contoured control panels on appliances as well as a wide variety of consumer products, including almost all electronic devices, medical devices, sports equipment and toys, et al. However, there are many restrictions on shape and base material and the dimensional control of pre-formed insert is important.

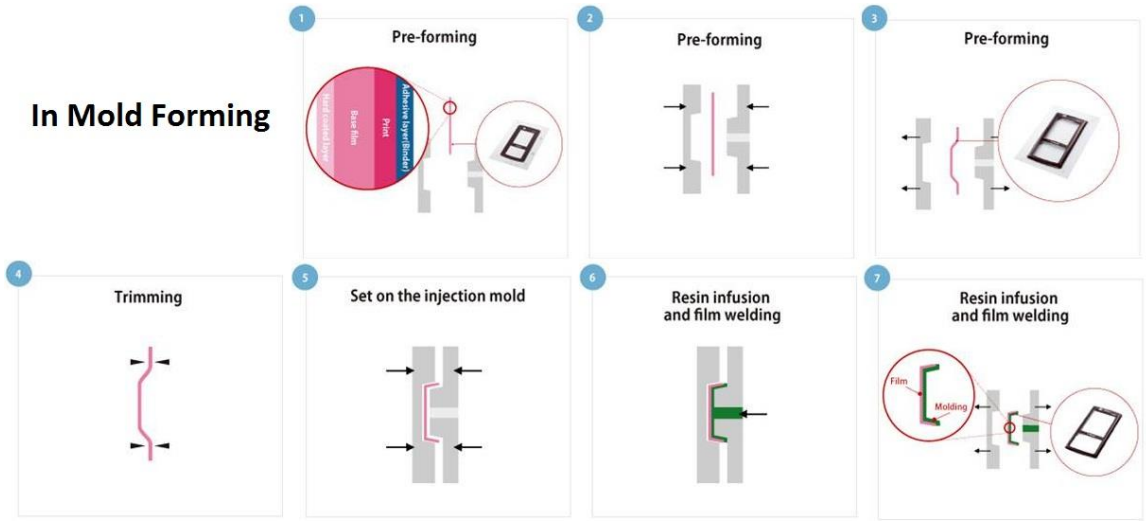

Figure 1-1 Process of in-mold forming (TORAY INDUSTRIES, 2014)

1.3 Motivation of Work

For the improvements sought by the automobile industry, much attention is being paid to paint replacement recently due to paint's poor durability, environmental stigma and high costs. Paints emit volatile organic compounds (VOCs) during curing, over 1500 tons of VOCs per year. Besides, paint application and assembly lines require large floor

space and are the most expensive step in the automobile production (Sherman and Lilli, 2004). Here, shape memory TPU films are envisioned for the replacement of automobile exterior and interior paint applications, using their shape memory effects to avoid common issues like scratches, chips, strains and other damaging elements from occurring. To ease the complexity of the process, work begins with laminating shape memory TPU films onto the plastic substrate meant for the finished part using a suitable adhesive (their multilayer structure is shown in **Figure 1-2**). Then through IMF or simply thermoforming, the laminate can be shaped for automobile interior/exterior parts. However, the shape memory effect of TPU layers may influence the dimensional control of pre-formed insert (or finished parts), therefore affecting quality of final automobile interior/exterior parts. So, the shape memory effects of TPU based laminates after pre-forming needs to be investigated.

Figure 1-2 Multilayer structure of TPU based laminate

1.4 Objectives

In this work, we will be focusing on a series of highly proprietary shape memory TPU films supplied by 3M Canada with different modulus or monomer ratios (isocyanates/ polyols). They will be bonded to different substrates using a pressure sensitive acrylic adhesive supplied by 3M. A major part of this thesis will focus on the measurement and investigation of recovery behavior of TPU based laminates after thermoforming.

The specific objectives of the study are:

1. To design a suitable and easy-controlled thermoforming method as a major process to thermoform TPU based laminates and identify their optimal forming conditions
2. To develop an effective and precise recovery measurement method to quantify the recovery behaviour of formed TPU based laminates that reflects the strain history of thermoforming
3. To study the influences of different film modulus, different substrates, and changing environmental temperature as well as deep draw values on the recovery behavior of TPU based laminates after thermoforming
4. To develop an analysis model to describe recovery behavior of formed TPU based laminates in order to have a better understanding of the data from experiments

Chapter 2 Literature Review

2.1 Shape Memory Polymer

Shape memory polymers (SMPs) are a special type of polymeric materials that inherently deform when external stimuli like electricity, magnetism, heat, moisture and light are applied (Behl and Lendlein, 2007, Behl et al., 2010, Leng and Du, 2012). The research interest in SMPs from all over the world has grown rapidly for their different applications since SMPs were discovered in 1980s. It's not unrealistic to say that the finding of shape memory properties in polymers was a milestone in the history of smart materials research. Recently, thermally responsive SMPs have drawn pronounced attention due to their unique behaviour by being able to recover their original shapes from heating, especially among the class of thermoplastic shape memory polyurethanes (TPUs) due to their versatile structure and mechanical properties (Behl et al., 2010). Actually, it is the discovery of thermally responsive shape memory effect in TPU (Leng and Du, 2012) that resulted in the most systematic knowledge on shape memory polymers.

2.2 Properties of SMPs

2.2.1 Shape Memory Properties

Diisocyanates, polyols and chain extenders are usually used as three basic monomeric components for the production of TPU, which is normally composed of two segments, i.e. soft and hard segments (Leng and Du, 2012). Usually, soft segments (reversible phase) are created by polyols such as polyester diols and long chain polyether diols, with the function of a reversible molecular switch. Meanwhile, hard segments (fixed phase) are generated by the reaction between diols/diamines and diisocyanates, capable of forming physical crosslinking that link soft segments together (Behl and

Lendlein, 2007, Behl et al., 2010, Leng and Du, 2012, Madbouly et al., 2007) (shown in **Figure 2-1**). Owing to the different polarity of soft and hard segments, the microphase-separated morphology in TPU is the key to their thermally responsive shape memory properties. The microphase-separated morphology influences this thermally responsive shape memory is based on the size and distribution of these phases, which can be modified by regulating soft and hard segments for the purpose of achieving optimal shape memory property of SMPs (Leng and Du, 2012).

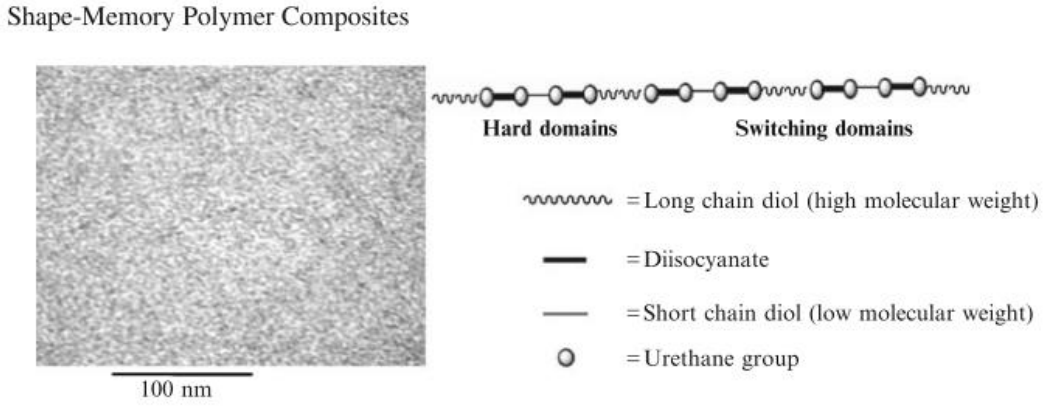

Figure 2-1 Schematic diagram of the hard and soft domains of PU structure. The TEM shows microphase separation morphology for the hard domains (dark particles) and soft domains (bright matrix) (Madbouly et al., 2007)

A higher content of hard segments will increase the modulus of a TPU (Leng and Du, 2012, Madbouly and Lendlein, 2010). The influence of hard segments on the microphase-separated morphology is mainly dependent on their molecular symmetry and structures; a better compatibility with soft segments tends to facilitate more hard segments dispersed in domains of soft segments, thus weakening the microphase separation (Chen and Schlick, 1990). In terms of soft segments, the microphase-separated morphology is mainly reliant on the interaction between polyols and other segments through their polarity and hydrogen bonds (Lee et al., 2004).

During the process of SMP shape memorization, temporary shapes can be created by deforming at a temperature above its lower transition temperature (T_{trans}) then being cooled down to a temperature below T_{trans} (Lee et al., 2004, Leng and Du, 2012). Later through heating SMPs above their T_{trans}, shapes can be recovered to their original shapes. Thus, as the temperature for switching on its shape memory behavior, T_{trans} is a crucial material property for SMP (Behl and Lendlein, 2007, Behl et al., 2010, Madbouly and Lendlein, 2010). Usually, based on the thermal transition of the soft segments, SMP can be categorized into two types: one is a SMP containing crystalline soft segments characterized by a melting temperature T_m (T_m-type SMPs, shown as **A** in **Figure 2-2**), while the other one is an SMP containing amorphous soft segments characterized by a glass transition temperature T_g (T_g-type SMPs, shown as **B** in **Figure 2-2**) (Leng and Du, 2012).

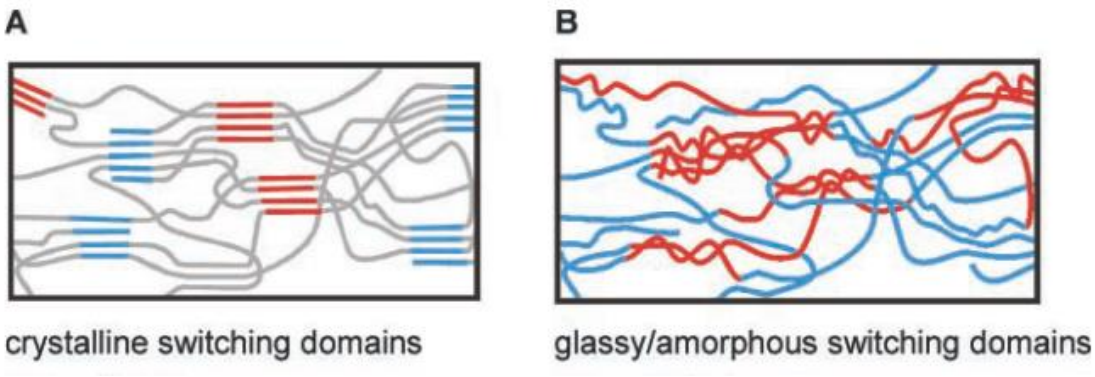

Figure 2-2 Different architectures for **(A)** crystalline switching segments and **(B)** amorphous switching segments (Behl et al., 2010)

The values of T_{trans} are mainly dependant on the flexibility of polymer chain – SMPs with more flexible chains usually having a lower value of T_{trans} (Fried, 2003). It can be tuned by chain length (Chun et al., 2007, Ji et al., 2011), side groups (Fried, 2003), branching (del R ó et al., 2011, Overney et al., 2000), cross-linking (del R ó et al., 2011,

Overney et al., 2000), molecular weight (Chen et al., 2007, Lin and Chen, 1998b, Rogulska et al., 2008) and monomer ratio (Oprea, 2009, Zhu et al., 2007). Normally, value of T_{trans} increases with increasing hard segment content (Leng and Du, 2012).

2.2.2 Physical and Mechanical Properties

Other than shape memory properties, several physical and mechanical properties of SMPs, like elastic modulus and viscosity are remarkably altered according to the changes of their temperature, especially at T_{trans} of SMPs. As is shown in **Figure 2-3** (Kim et al., 1998), SMPs, namely PCL4000- and PCL8000-based TPU, clearly exhibit a sharp transition from glass phase to rubber phase when they were heated across their T_{trans} around 50°C (T_m of the soft segment). Meanwhile, PCL2000-based PU (non-SMPs) showed a broad transition instead due to the fact that the PCL segments couldn't crystallize below a molecular weight limit of 2000-3000 (Kim et al., 1998).

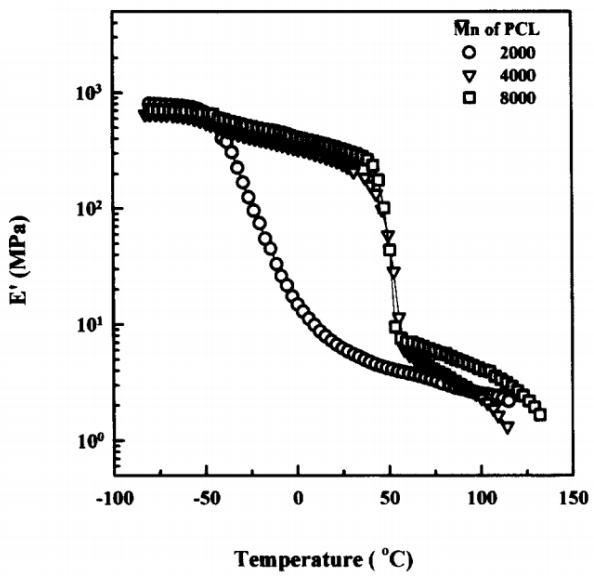

Figure 2-3 Effect of PCL molecular weight on the storage modulus of PU ionomers with 70% soft segment content (Kim et al., 1998)

2.3 Measurement and Analysis of SMPs' Shape Memory Behaviour

2.3.1 Under In-plane Deformations

The quantitative measurement and analysis of SMPs' shape memory behaviour can be carried out in thermo-mechanical cycle tests. The values of strain fixing and recovery measured in thermo-mechanical cycle tests are the most common quantification for SMPs' shape memory behaviour. Each single cycle contains two parts, a programming part and a recovery part; former is the fixing of SMPs' temporary shapes and the latter is the recovery process to their permanent shapes (Lendlein and Kelch, 2002b). A variety of testing protocols are used in the programming part (Leng and Du, 2012). Cooling can be implemented under stress-control or strain- control (Choi and Lendlein, 2007). The stress change on the samples $\sigma(t)$ is recorded in strain-controlled tests while the strain change $\varepsilon(t)$ is recorded in stress-controlled tests. Meanwhile, various recovery modes are applied. In the stress-free recovery condition, T_{trans} of SMPs can be measured at the inflection point in the stain-temperature $\varepsilon(T)$ curve (Kelch et al., 2007) while in the constant strain ($\varepsilon(t)$=constant) condition, the maximum stress σ_{max} created in the recovery and the corresponding temperature $T_{\sigma,\ max}$ can be measured in the stress-temperature $\sigma(T)$ curve (Gall et al., 2005, Liu et al., 2003). The impact of testing parameters such as heating and cooling rates, strain rate, deformation temperature T_{deform}, fixation temperature for temporary shape T_{low} and recovery temperature for the original permanent shape T_{high} on the shape memory behaviour of SMPs have been investigated (Gall et al., 2005, Leng and Du, 2012, Liu et al., 2003). A summary of the possible combinations of programming and recovery moduli leading to different types of cycle tests is given in **Table 2-1** below.

Table 2-1 Definition of cycle types on thermo-mechanical tensile tests for characterization of the shape memory behaviour (Leng and Du, 2012)

Cycle Type	Programming Module	Recovery Module

	$T_{deform} < T_{trans}$	$T_{\sigma,\ max}$	$T_{deform} > T_{trans}$; $T_{\sigma,\ maxb}$	$T_{high} > T_{trans}$; $T_{\sigma,\ max}$	Results
A.1	Stain-controlled	Deformation to ε_m	Deformation to ε_m; cooling to T_{low} under $\varepsilon = \varepsilon_m$	Stress free: σ=0MPa	T_{trans}
A.2				Constant strain: $\varepsilon = \varepsilon_m$	σ_{max}; $T_{\sigma,\ max}$
A.3				Stress free: σ=0MPa	T_{trans}
A.4				Constant strain: $\varepsilon = \varepsilon_m$	σ_{max}; $T_{\sigma,\ max}$
B.1	Stress-controlled	Deformation to σ_m	Deformation to ε_m; determining σ_m cooling under $\varepsilon = \varepsilon_m$=constant	Stress free: σ=0MPa	T_{trans}
B.2				Constant strain: $\varepsilon = \varepsilon_m$	σ_{max}; $T_{\sigma,\ max}$
B.3				Stress free: σ=0MPa	T_{trans}
B.4				Constant strain: $\varepsilon = \varepsilon_m$	σ_{max}; $T_{\sigma,\ max}$

Note: Each cycle consists of a programming and recovery part.

In thermo-mechanical cycle tests, the cycle is usually repeated 3-5 times. The first cycle is used to eliminate the previous thermo-mechanical history on SMPs and the subsequent 2-5 cycles are applied as the measurement of the shape memory behaviour of SMPs. The results of above thermo-mechanical cycle tests can be expressed by a ε-σ curve shown in **Figure 2-4 (a)**. A short-coming of the ε-σ diagram is lack of information on T_{trans} based on this 2-D plot (Leng and Du, 2012). The 3-D diagram in **Figure 2-4 (b)** reveals more information (Lendlein and Kelch, 2002b). The ε-σ-T diagram presenting a thermo-mechanical cycle test combining stress-controlled programming and stress-free recovery that can not only provide the T_{trans} but also supplying other information like elastic modulus of SMPs at T_{high} and T_{low} (Leng and Du, 2012).

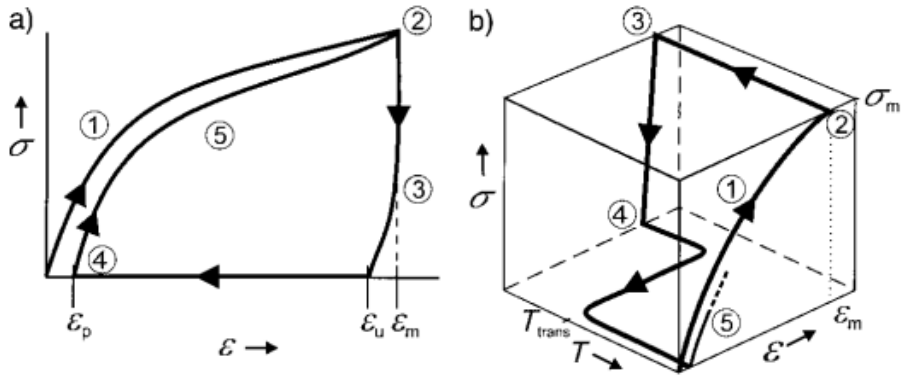

Figure 2-4 Schematic representation of the results of the cyclic thermo-mechanical investigations for two different tests: **(a)** ε-σ diagram: ①-stretching to ε_m at T_{high}; ②-cooling to T_{low} while ε_m is kept constant; ③-clamp distance is driven back to original distance; ④-at ε= 0% heating up to T_{high}; ⑤-start of the second cycle. **(b)** ε-σ-T diagram: ①-stretching to ε_m at T_{high}; ②-cooling down to T_{low} with cooling rate k_{cool} =dT/dt while σ_m is kept constant; ③-clamp distance is reduced until the stress-free state σ=0 MPa is reached; ④-heating up to T_{high} with a heating rate k_{heat} =dT/dt at σ=0 MPa; ⑤-start of the second cycle (Lendlein and Kelch, 2002b)

As the two most common parameters for quantifying shape memory properties of SMPs, the strain recovery rate R_r and the strain fixity rate R_f can be measured from thermo-mechanical cycle tests according to Equations **(2-1)** and **(2-2)** for the strain-controlled programming protocol and Equations **(2-3)** and **(2-4)** for the stress-controlled programming case (Leng and Du, 2012). R_r measures the ability of SMPs to recovery their permanent (original) shape while R_f describes the ability of the switching segments to fix the temporary deformation during the thermo-mechanical cycle tests (Behl et al., 2010). Ideally, smart application requires SMPs with a high percentage of R_r and R_f.

$$R_r(N) = \frac{\varepsilon_m - \varepsilon_p(N)}{\varepsilon_m - \varepsilon_p(N-1)} \quad \textbf{(2-1)}$$

$$R_f(N) = \frac{\varepsilon_u(N)}{\varepsilon_m} \quad \textbf{(2-2)}$$

$$R_r(N) = \frac{\varepsilon_1(N) - \varepsilon_p(N)}{\varepsilon_1(N) - \varepsilon_p(N-1)} \quad \textbf{(2-3)}$$

$$R_f(N) = \frac{\varepsilon_u(N)}{\varepsilon_1(N)} \quad \textbf{(2-4)}$$

2.3.2 Under Out-of-plane Deformations

Nowadays, most of the measurements and analyses of SMPs' shape memory behaviours have been limited on small, uniaxial and in-plane deformations. However, nearly all practical applications of SMPs involve large, 3D and out-of-plane deformations which need more complex engineering analysis and design. Some efforts have been made to quantify and analyze the shape memory behavior of SMPs after bending (Lan et al., 2009, Lin and Chen, 1998a, Lin and Chen, 1998b, Zhang et al., 2014). In the work of Leng (Lan et al., 2009, Zhang et al., 2014), shape memory behavior of thermoset styrene-based SMP composite reinforced by carbon fiber fabrics was investigated through a bending shape recovery test shown in **Figure 2-5** (Lan et al., 2009). The value of the shape recovery ratio was calculated by Equation **(2-5)**, where R_N represented the shape recovery ratio of the N_{th} thermo-mechanical bending cycle (Lan et al., 2009).

$$R(N) = \frac{\theta_0 - \theta_N}{\theta_0} \times 100\% (N = 1, 2, 3, ...) \quad \textbf{(2-5)}$$

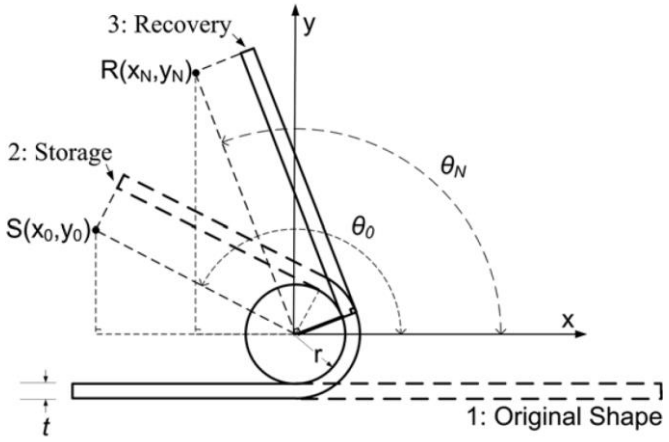

Figure 2-5 Schematic illustration of the setup for the shape recovery performance test (Lan et al., 2009)

Furthermore, in order to reinforce the mechanical strength and stiffness of SMPs for more applications in the engineering industry, a few efforts have been made to investigate the shape memory behaviour of composite SMPs (Jeong et al., 2000, Liang et al., 1997, Lin and Chen, 1998b) and SMPs based laminates (Zhang and Ni, 2007). For the purpose of stiffness reinforcement, Zhang et al (Zhang and Ni, 2007) fabricated laminations of carbon fiber fabric and SMPs sheets. The bending recoverability of laminates was measured by Zhang, as shown in **Figure 2-6 (a)**. The bending recovery ratio (R) was expressed by Equation **(2-6)**, where ω_0 represented as the recovery deflection and ω_R represented as the initial deflection as shown in **Figure 2-6 (b)**. However, to the best of our knowledge, there is little reference on the assessment of the shape memory behavior under more applicable conditions such as a thermoforming process where large scale stretching as well as bending occur simultaneously.

$$R = \frac{\omega_R}{\omega_0} \times 100\% \qquad \textbf{(2-6)}$$

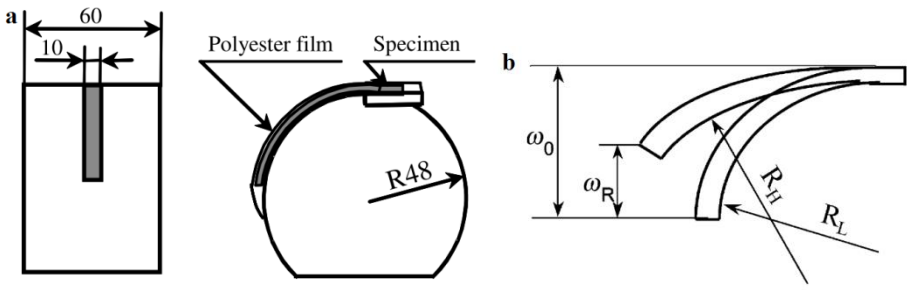

Figure 2-6 The jig for fixing specimen shape **(a)** and the definition of bending recovery ratio **(b)** (Zhang and Ni, 2007)

2.4 Modelling of SMPs' Shape Memory Behaviour

2.4.1 Background

Before describing the modelling methods of shape memory behaviour, its mechanism needs to be briefly described. For the purpose of modelling, it is generally

believed that shape memory behaviour for an SMP is due to the transition of a cross-linked polymer from glassy to rubbery phase as temperature increases across T_{trans} (Leng and Du, 2012). The underlying physical mechanisms have been discussed deeply by Lendlein et al (Lendlein and Kelch, 2002a), Liu et al (Liu et al., 2006) and Qi et al (Qi et al., 2008). Generally, models developed based on the above mechanism are considered as constitutive and can be classified into two categories: phase transition type and viscoelasticity type (Leng and Du, 2012). For the phase transition type, SMPs are considered as a mixture containing both glassy and rubbery phases and a large amount of work has been done by Liu et al (Liu et al., 2006), Chen and Lagoudas et al (Chen and Lagoudas, 2008a, Chen and Lagoudas, 2008b), Qi et al (Qi et al., 2008) and so on. Later there was an additional concept of storage deformation introduced (Chen and Lagoudas, 2008a, Chen and Lagoudas, 2008b, Liu et al., 2006) which further categorized the phase transition type into two branches: models based on phase transition and models based on storage deformation. In terms of the second type, viscoelasticity, viscosity and elastic modulus were all considered as nonlinear functions of temperature across T_{trans} and treated as a means to extend the standard linear viscoelastic (SLV) model as the constitutive model for SMPs. This model type has been well developed by Tobushi et al (Tobushi et al., 1997, Tobushi et al., 2001), Ngnyen et al (Nguyen et al., 2008) and so on. For the modeling of complex 3D, out-of-plane deformation of SMPs, finite element analysis still needs to be applied (Leng and Du, 2012). Based on the mechanics analysis of different layers, modeling SMPs based laminates can be achieved (Zhang and Ni, 2007), however, little research has been made on the field. In this literature review, only models based on viscoelasticity were reviewed.

2.4.2 Models Based on Viscoelasticity

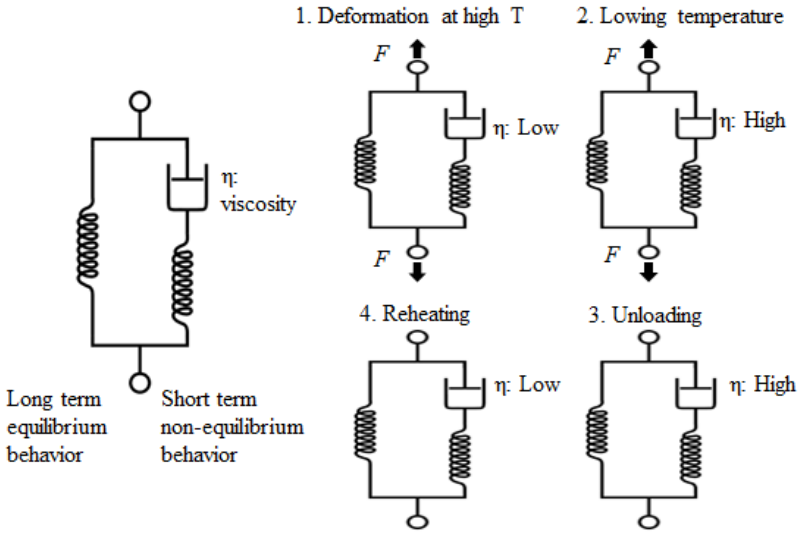

Figure 2-7 Schematic of the shape memory effect due to the dramatic change of viscosity in shape memory polymers (Leng and Du, 2012)

It was realized that the shape memory behavior in SMPs is because of the significant differences in their viscosity, modulus or relaxation time when the temperature goes across T_{trans} (Leng and Du, 2012). This point of view has been brought into the constitutive models of SMPs to describe their shape memory behavior recently. As shown in the left of **Figure 2-7**, the left element denotes the long-term equilibrium response of SMPs and the right Maxwell element denotes the non-equilibrium response. Normally, compared with the non-equilibrium spring in the Maxwell element, the equilibrium spring in the left has a much lower stiffness. With the increase of temperature, due to a very low viscosity of dashpot, non-equilibrium spring is not activated because of the highly extension of the dashpot which will accommodate most deformation. When the temperature falls below T_{trans}, an extremely long relaxation time of SMPs will be generated due to the dramatic increase of viscosity in the dashpot. Shown in the right bottom of **Figure 2-7**, the equilibrium will be achieved through the balance of above two

springs after the withdrawal of the load with a small amount of recovery because of the high modulus of the spring in Maxwell element. The shape recovery behavior with respect to increasing temperature is achieved by decreasing the viscosity term of the dashpot (Leng and Du, 2012, Tool, 1946).

Initially, a 1-D constitutive model was developed by Tobushi et al (Tobushi et al., 1997, Tobushi et al., 2001) based on viscosity captures well the shape memory behavior of SMP. Its ε-σ relationship was determined through the modification of the standard linear viscoelastic model (SLV) as shown in Equation **(2-7)**,

$$\dot{\varepsilon} = \frac{\dot{\sigma}}{E} + \frac{\sigma}{\eta} - \frac{\varepsilon - \varepsilon_S}{\tau_r} + \alpha \dot{T} \qquad \textbf{(2-7)}$$

where ε and σ are the stress and the strain; E, η and τ_r are the elastic modulus, the viscosity and the relaxation time, respectively; α and $\dot{T}$ are the thermal expansion coefficient and the temperature (Tobushi et al., 1997, Tobushi et al., 2001).

The ε_s introduced in the work of Tobushi *et al* represented the non-recoverable strain related to shape memory behaviour of SMPs, which is shown as

$$\varepsilon_S = \begin{cases} 0 & (\varepsilon_c < \varepsilon_1) \\ C(\varepsilon_c - \varepsilon_1) & (\varepsilon_c > \varepsilon_1) \end{cases} \qquad \textbf{(2-8)}$$

where ε_c is a creep strain; ε_1 is a critical stain; C is a proportional coefficient. Both C and ε_1 are functions of temperatures (Tobushi et al., 1997, Tobushi et al., 2001),

$$C = C_g \exp\left\{ a_c \left(\frac{T_g}{T} - 1 \right) \right\} \qquad \textbf{(2-9)}$$

$$\varepsilon_1 = \varepsilon_g \exp\left\{ -a_\varepsilon \left(\frac{T_g}{T} - 1 \right) \right\} \qquad \textbf{(2-10)}$$

where C_g, ε_g, a_c *and* a_ε are constants. Besides, E, η and τ_r are functions of temperature following the similar functional form of C (Tobushi et al., 1997, Tobushi et al., 2001).

The short-coming of Tobushi model is the unclear contributors to ε_s. Later, a thermo-viscoelastic model was developed by Nguyen et al (Nguyen et al., 2008) based on combining the glass-forming process. This model considered a significant reduction could occur in chain mobility of macromolecules as well as free volume when the temperature was below T_{trans}. Combining Hodge-Scherer equation and an Erying-type viscous flow rule (Nguyen et al., 2008), the relationship between viscosity vs. time and temperature can be expressed as

$$\eta = \eta_0 \frac{Q}{T}\frac{S}{S_y}\exp\left\{\frac{C_1}{0.433}\left(\frac{C_2(T-T_f)+T(T_f-T_g^{ref})}{T(C_2+T_f-T_g^{ref})}\right)\right\}\left[\sinh\left(\frac{Q}{T}\frac{S}{S_y}\right)\right]^{-1} \qquad \textbf{(2-11)}$$

where η_0 is the viscosity at a reference temperature (typically the T_g) T_g^{ref} ; T_f is the fictitious temperature used in the work of Tool (Tool, 1946); Q is an activation parameter; S is the flow stress; S_y is the athermal shear resistance and characterizes the yielding behavior of polymers at low temperature; C_1 and C_2 are the two parameters from the WLF equation (Nguyen et al., 2008).

The viscous flow rule can then be described as

$$\dot{\gamma}^V = \frac{Q}{T}\frac{S_y}{\sqrt{2}\eta_0}\exp\left\{\frac{C_1}{0.433}\left(\frac{C_2(T-T_f)+T(T_f-T_g^{ref})}{T(C_2+T_f-T_g^{ref})}\right)\right\}\left[\sinh\left(\frac{Q}{T}\frac{S}{S_y}\right)\right] \qquad \textbf{(2-12)}$$

Chapter 3 Experimental

3.1 Materials

Eight experimental shape memory polyurethane (TPU) films were supplied by 3M Corporation (Canada). Among the eight, three of them were transparent and colorless made from polymers synthesized with different monomer ratios (isocyanate-polyol ratios, MR), MR=0.8, 0.95 and 1.05 and they are designated as Transparent TPU-0.8, Transparent TPU-0.95 and Transparent TPU-1.05. The remaining five were black and opaque in nature. Among the five black TPU films, three of them had the same thickness of 0.2mm with different modulus and they were designated as Black TPU-Low, Black TPU-Med and Black TPU-High; the other two had different roughnesses on their surfaces and they are designated as Black TPU-Glossy and Black TPU-Mat (the later contains adhesive layer on the underside). The majority of studies, particularly the detailed examination of recovery were only performed with Black TPU-Low, Black TPU-Med and Black TPU-High.

Polypropylene sheets (purchased from DuPont with thickness of 0.5mm) and ABS sheets (purchased from McMaster-Carr with thickness of 0.5mm) were used as substrates for the lamination. The adhesive used was 3M Adhesive Transfer Tape 468MP, a high shear strength pressure sensitive adhesive with thickness of 0.125 mm (named as TT in abbreviation).

3.2 Lamination

The TPU films with adhesive layers were laminated to either PP or ABS substrates using a HL-100 hot roll laminator (Chemsultants International; Cincinnati,

OH) equipped with a top metal roller and a lower rubber roller. The holding line pressure on the top roller of the laminator and the nip gap opening were kept constant at 25psi (276 kPa) and 90% of sample thickness, respectively for all laminates being prepared. Lamination was done at 23°C using a roller speed of 5 mm/s. After three passes through the laminator to ensure uniform adhesion, each laminate was placed on a flat surface for 72h to cure. After that, laminates were cut to be dog-bone shaped tensile specimens (125mm (length) × 12.7mm (width) × 0.83 mm (thickness)) according to ASTM D-1822-12 before thermoforming.

3.3 Thermoforming

A modeled thermoforming process based on matched-mold forming was used to create a desired arched shape in the laminates in order to investigate their recovery behaviour in an easily controlled way. The thermoforming was conducted inside a controlled environmental chamber attached to a 5 kN universal mechanical testing system (UMTS) supplied by the Instron Corporation (Canton, MA, USA). The deformation was produced in this case included bending and stretching modes by using a male-female conforming die set featuring an arch of 26mm radius, as shown in the left of **Figure 3-1**.

Figure 3-1 (right) shows the mold which had sufficient space for three samples to be formed simultaneously for the purposes of assessing experimental uncertainty. The samples were initially heated up to 160^{o}C by setting the chamber temperature to 180^{o}C. The forming process was started with a controlled out-of-plane deformation rate of 25mm/min to a specified depth which gave the sample a constant strain and initial central angle for recovery observation. Both mold and samples were then immediately moved to

a deep freezer (Rototron Corporation) with an ambient temperature of -40°C. Once cooled down to 10°C over a span of 20 minutes, the upper male-half of the mold was

Figure 3-1 Matched molds used in the forming process (left) and thermoforming process inside the environmental chamber (right)

raised and the three specimens were trimmed, and then removed. The short end of the trimmed sample was sealed with epoxy adhesive to minimize delamination. Minimal direct contact occurred while performing these steps to minimize any rise in sample temperature till the recovery test could be started.

3.4 Recovery Study

3.4.1 New Recovery Measurement

The arch-molded laminates were clamped on one end into a fixture while still at 10°C and then moved to a dry temperature-regulated chamber for recovery, as shown in **Figure 3-2**.

The arch-molded laminates were fixed at one end and set in a vertical position to avoid frictional restraint during the recovery yet also minimize the influence of body forces. During the recovery phase of the test, the unfixed end of the formed laminate

freely traversed (see in **Figure 3-3**) from its original position A to a position B and eventually would arrive at position C if it could fully recover, changing the central angle from initial angle α to β to eventually 0^o. The recovery curve (blue and red curve) is the

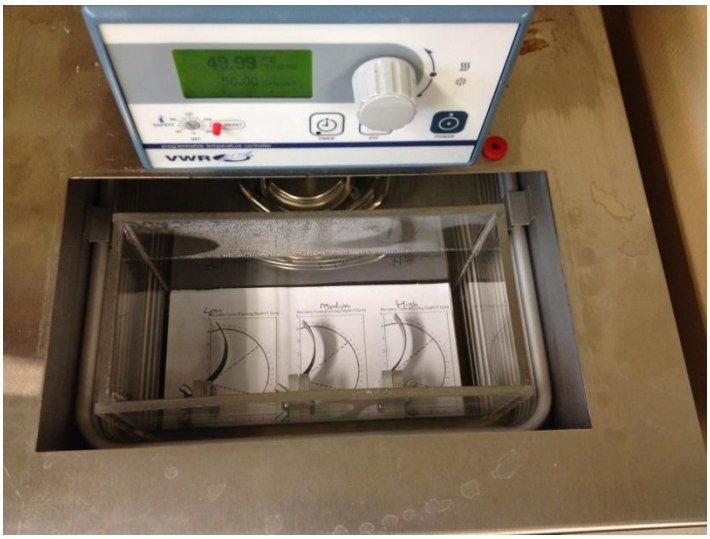

Figure 3-2 Temperature regulated recovery chamber using a digitally controlled circulating water bath

track of the unfixed end of formed laminate which is calculated through MATLAB (code was provided in **Appendix A**) based on following two assumptions during the recovery process: (1) the arc length of laminates was constant; and (2) formed laminate recovered along the path of a circular arc with changing central angle. Printed curves with demarcations showing the central angle were placed on the floor of the chamber with the affixed specimens appropriately positioned. Images were auto-taken every 15s for the first 30 minutes as the sample temperature rose from 10^oC to the set temperature and then every 1min for 30min using cameras placed on top of the recovery chamber closed with a transparent PMMA panel. After that first hour had past, a more heavily insulated lid (original lid of the circulating bath) replaced the acrylic lid of the circulating bath to prevent water in the bath from evaporating during the overnight measuring period. With the insulated lid the recovery angles could only be observed momentarily by removing

for progressively longer durations until the final angle was recorded after 24 hours. The recovery nature of a TPU based laminate was reported as its angle recovery ratio [$R_a(t)$, %] which was defined by the following Equation **(3-1)**:

$$R_a(t) = \frac{\alpha(0) - \alpha(t)}{\alpha(0)} \times 100\% \qquad \textbf{(3-1)}$$

where $\alpha(0)$ is the initial central angle after forming and $\alpha(t)$ is the central angle of formed laminate at time t. A value of R_a = 100% meant that the laminate had fully recovered to its original flat shape. As the major part of both TPU and substrates' stress relaxation was completed in the first 5 minutes (shown in **Figure 4-9** and **Figure 4-10**), the secant slope of $R_a(t)$ vs. t curve for the first 5 minutes of recovery was used to define the recovery rate.

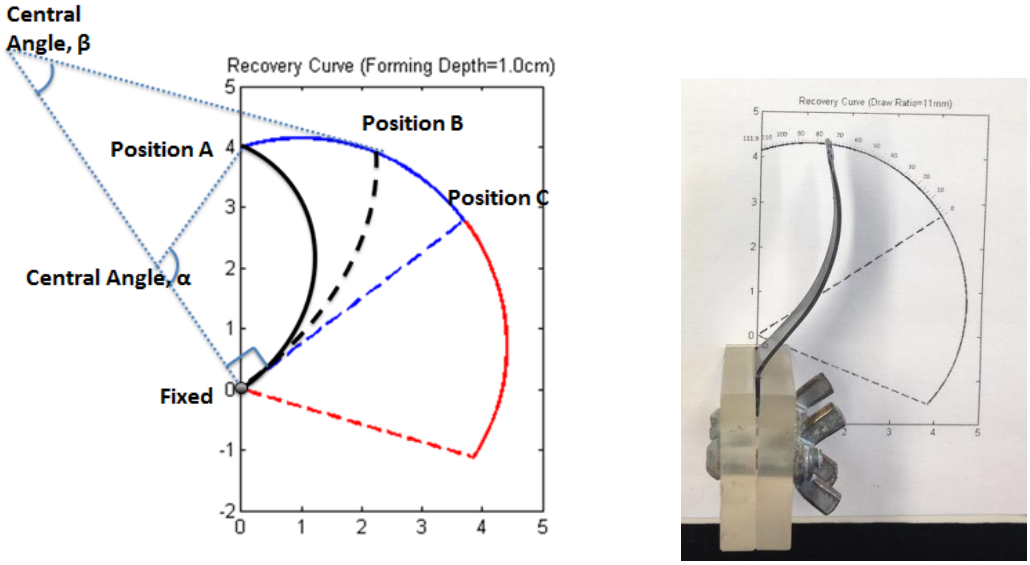

Figure 3-3 New recovery measurements for the recovery process of formed laminate (left) and the actual sample during the recovery measurement (right)

3.4.2 Influence of SMP's Properties on Recovery Behaviour of Laminate

The three TPU films with different moduli, Black TPU-Low, TPU-Med and TPU-High were studied for their recovery behavior as arch-molded TPU based laminates based on the recovery measurement method discussed in **Section 3.4.1**. PP was used as the

substrate (with TT adhesive used for all experimental runs) and ambient recovery temperature was fixed at 45°C. Deep draw value of the upper mold was fixed at 10mm which gave the laminate a strain of 18.25% and 106° as the initial central angle. Through the recovery measurement, angle recovery ratio curves ($R_a(t)$ vs. t) of laminates with the three TPU films were generated. Each condition was measured for at least five repeats.

3.4.3 Influence of Substrates' Properties on Recovery Behaviour of Laminate

As one of the most common engineering plastics, ABS was used as an alternative substrate to study recovery behavior of TPU based laminates, in this case with different interfacial and mechanical properties compared to PP. Ambient recovery temperature and deep draw value were fixed at 45°C and 10mm, respectively. Through the recovery measurement, angle recovery ratio curves ($R_a(t)$ vs. t) of laminates with the three TPU films affixed to ABS were generated and compared to the results for PP. Each condition was measured for at least five repeats.

3.4.4 Influence of Recovery Temperature on Recovery Behaviour of Laminate

Two additional ambient recovery temperatures were examined, namely 15°C and 65°C to investigate the effect of environmental conditions on the recovery behavior of TPU based laminates. PP was used as the substrate layer in the laminate while Black TPU-Low, TPU-Med and TPU-High were used as TPU layers. The deep draw value was fixed at 10mm. Angle recovery ratio curves ($R_a(t)$ vs. t) of laminates with different TPU films were generated, with at least five repeats for each curve.

3.4.5 Influence of Draw on Recovery Behaviour of Laminate

Four additional deep draw values were tested, namely 6mm (81° as the initial central angle), 8mm (94°), 11mm (112°) and 12mm (117°) to investigate the effect of

total strain on the recovery behavior of TPU based laminates. As most of Black TPU-Low and Black TPU-Med layer in the TPU based laminate will be broken when the deep draw value was enhanced to 11mm and 12mm, only 6mm and 8mm were applied for TPU based laminates using Black TPU-Low and Black TPU-Med.

3.5 Characterization

3.5.1 Differential Scanning Calorimetry

The thermal transition temperatures of all TPU films (Transparent TPU-0.80, TPU-0.95 and TPU-1.05, Black TPU-Glossy, TPU-Mat, TPU-Low, TPU-Med and TPU-High) were obtained by differential scanning calorimetry (DSC) at a heating rate of 10^{o}C/min from -25^{o}C to 225^{o}C, using a model Q200 (TA instruments, New Castle, USA). Three consecutive cycles of heating-cooling were carried out for all the samples. All tests were done under a 50 mL/min flow of nitrogen.

3.5.2 Dynamic Mechanical Analysis

The variation in modulus of the material with respect to temperature was obtained by dynamic mechanical analysis (DMA) on all TPU films (Transparent TPU-0.80, TPU-0.95 and TPU-1.05, Black TPU-Glossy, TPU-Mat, TPU-Low, TPU-Med and TPU-High) and two substrates (PP and ABS) with a DMA 2980 (V1.7B), TA instruments, using liquid N_2 as the cooling medium. The temperature sweep was done at a fixed frequency of 10 Hz, an amplitude of 100 μm from -25 ℃ to 120 ℃ (or -25 ℃ to 180 ℃ for PP and ABS) using a ramp of 5 ℃/min. The test was conducted on rectangular specimens of 30mm × 6mm dimension by mounting them in a film tension clamp with a pretension of 0.01 N. The dynamic storage modulus (G'), loss modulus (G'') and tan delta were

recorded for a temperature range of -25 to 120 ℃ for TPU films and -25 ℃ to 180 ℃ for PP and ABS.

3.5.3 Tensile Test: Stress-strain Behaviour

Dog-bone shaped tensile specimens with 40mm gauge length were prepared according to ASTM D-1822-12. Dimensions differed based on whether a film or substrate was being tested, namely 125mm (length) × 12.7mm (width) × 0.145-0.258 mm (thickness) [films] versus 125mm (length) × 12.7mm (width) × 0.500 mm (thickness) [substrates]. Tensile test were carried out using a bench-top universal mechanical testing system (UMTS), Model 3366 supplied by the Instron Corporation (Canton, MA, USA) attached with a controlled environmental chamber (HeatWave oven). A constant cross-arm speed of 200mm/min was used. All TPU films were tested at two different temperature viz., 22-23°C (RT) and 150°C (HT). The black TPU-Low, TPU-Med and TPU-High films as well as the two substrates, PP and ABS, were also tested at temperatures of 45°C and 65°C which corresponded to the shape memory recovery study conditions.

3.5.4 Relaxation Test: Stress Relaxation Behaviour

Stress relaxation tests were carried out using the bench-top UMTS at a constant strain of 10% (3% for ABS) and constant cross-arm speed of 12mm/min for three different temperatures viz., 22-23°C (RT), 45°C and 65°C. Three types of TPU films (Black TPU-Low, TPU-Med and TPU-High) of 152.4mm x 25.4mm x 0.2mm dimensions, PP and ABS sheets of 152.4mm x 25.4mm x 0.5mm dimensions were tested using a 100mm gauge length (i.e. grip-to-grip distance). The relaxation time was computed using a standard linear viscoelastic model (SLV, as shown in **Figure 3-4** and

Equation **2**) based on regression fitting of the stress relaxation data. The upper element in **Figure 3-4** (E_{1a}) represents the long-term equilibrium response of the TPU films and the bottom Maxwell element (E_{1b}) represents the non-equilibrium response. Normally, the spring in the Maxwell element has a much higher stiffness than the equilibrium spring.

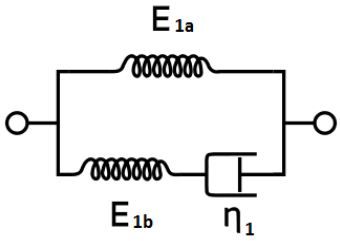

Figure 3-4 Standard linear viscoelastic (SLV) model(Leng and Du, 2012)

$$\dot{\sigma} + \frac{E_{1b}}{\eta_1}\sigma - \frac{E_{1a}E_{1b}}{\eta_1}\varepsilon = (E_{1a} + E_{1b})\dot{\varepsilon} \qquad (\mathbf{2})$$

In the test of stress relaxation, $\dot{\varepsilon}$ =0 and ε =10%. After integration, the equation is:

$$\sigma = 0.1E_{1a} + C\exp(-t/\tau) \qquad (\mathbf{3})$$

where $\tau = \eta_1 / E_{1b}$ is the relaxation time of samples (min) and E_{1a} and *C* are constants in this equation.

Chapter 4 Characterization

4.1 Differential Scanning Calorimetry

The DSC thermograms recorded during the first and second heating cycle are shown in **Figure 4-1**. The TPU samples showed a glass-transition temperature (T_g) at 19-25 ℃, which corresponded to the T_g of the soft-segments (polyether-segments) of the polyurethane, **Figure 4-1 (a)**. A variation in the T_g values by 2-4 ℃ was noticed for the same samples during the second heating cycle, which could be because of the thermal and processing history imposed on the samples, **Figure 4-1 (b)**. There was no observable melting endothermic peak till 225 ℃. This indicates that the samples do not have any higher order structure at higher temperatures in the samples.

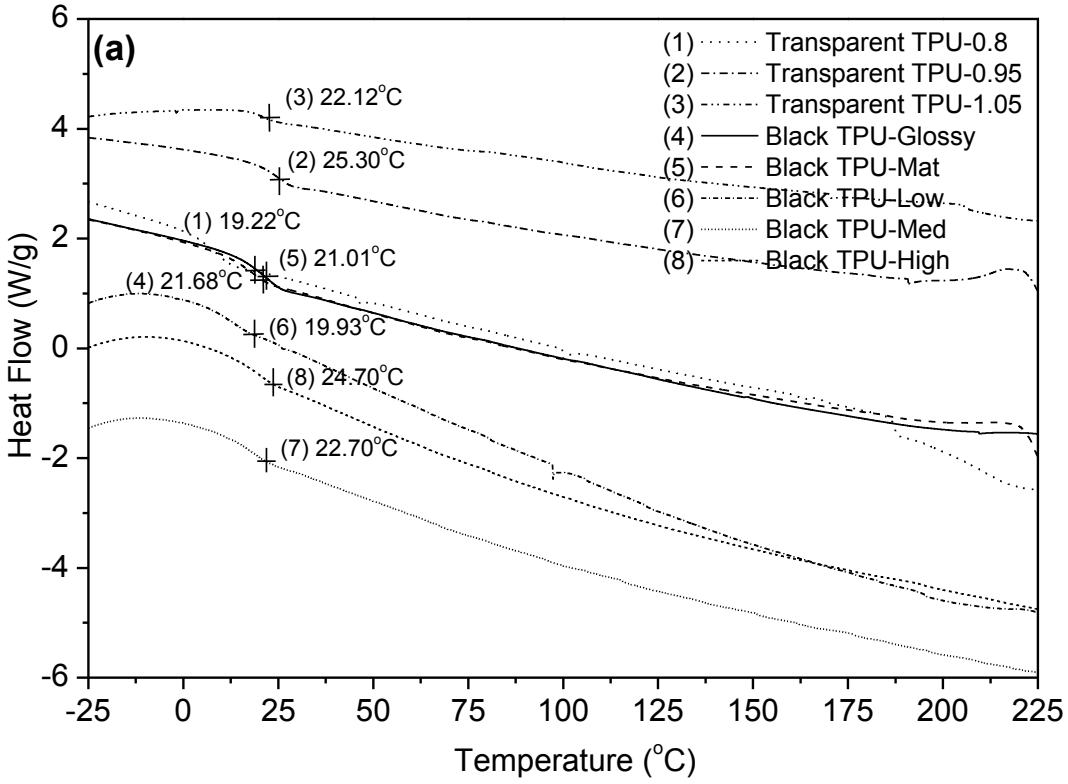

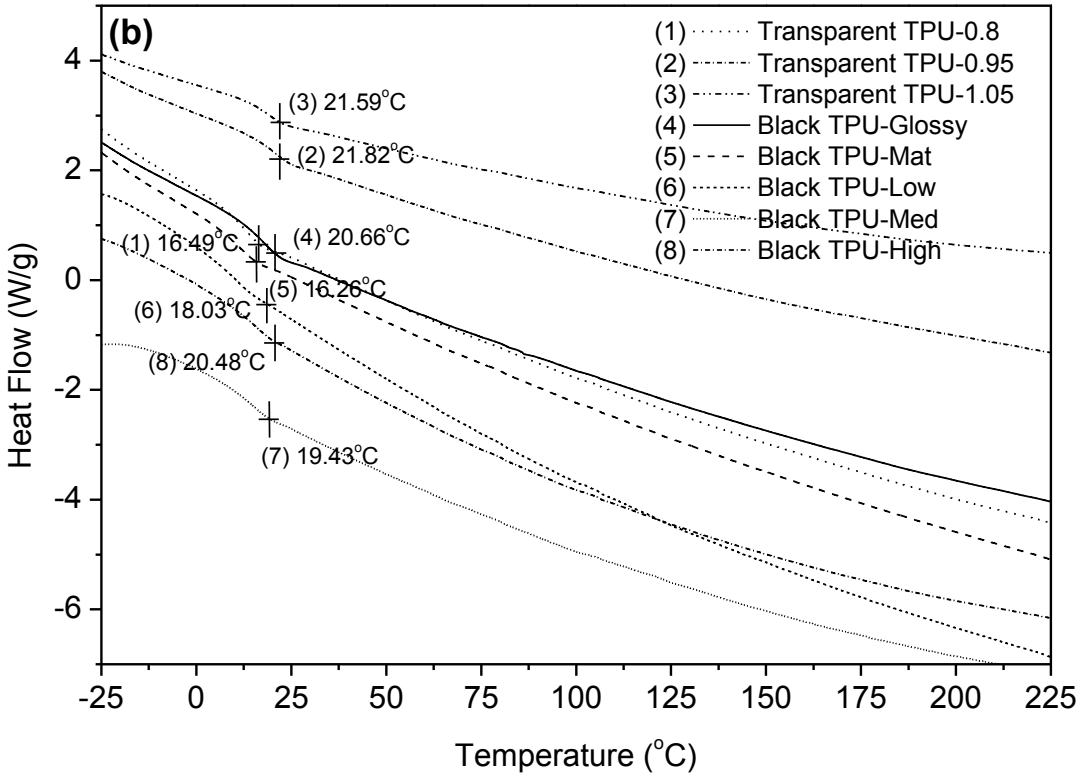

Figure 4-1 DSC curves of the all TPU films **(a)** First heating **(b)** Second heating

4.2 Dynamic Mechanical Analysis

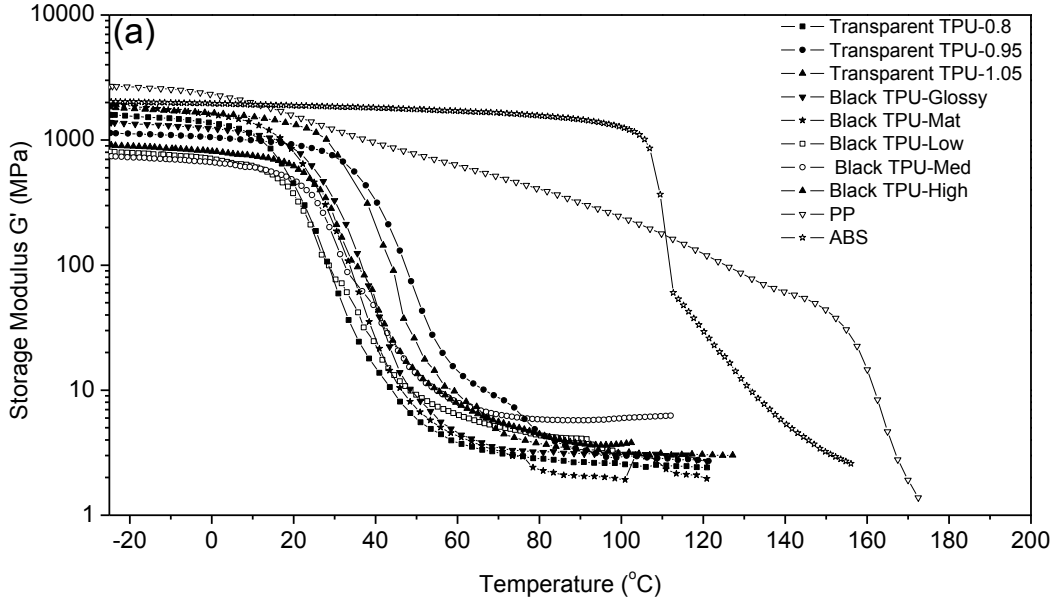

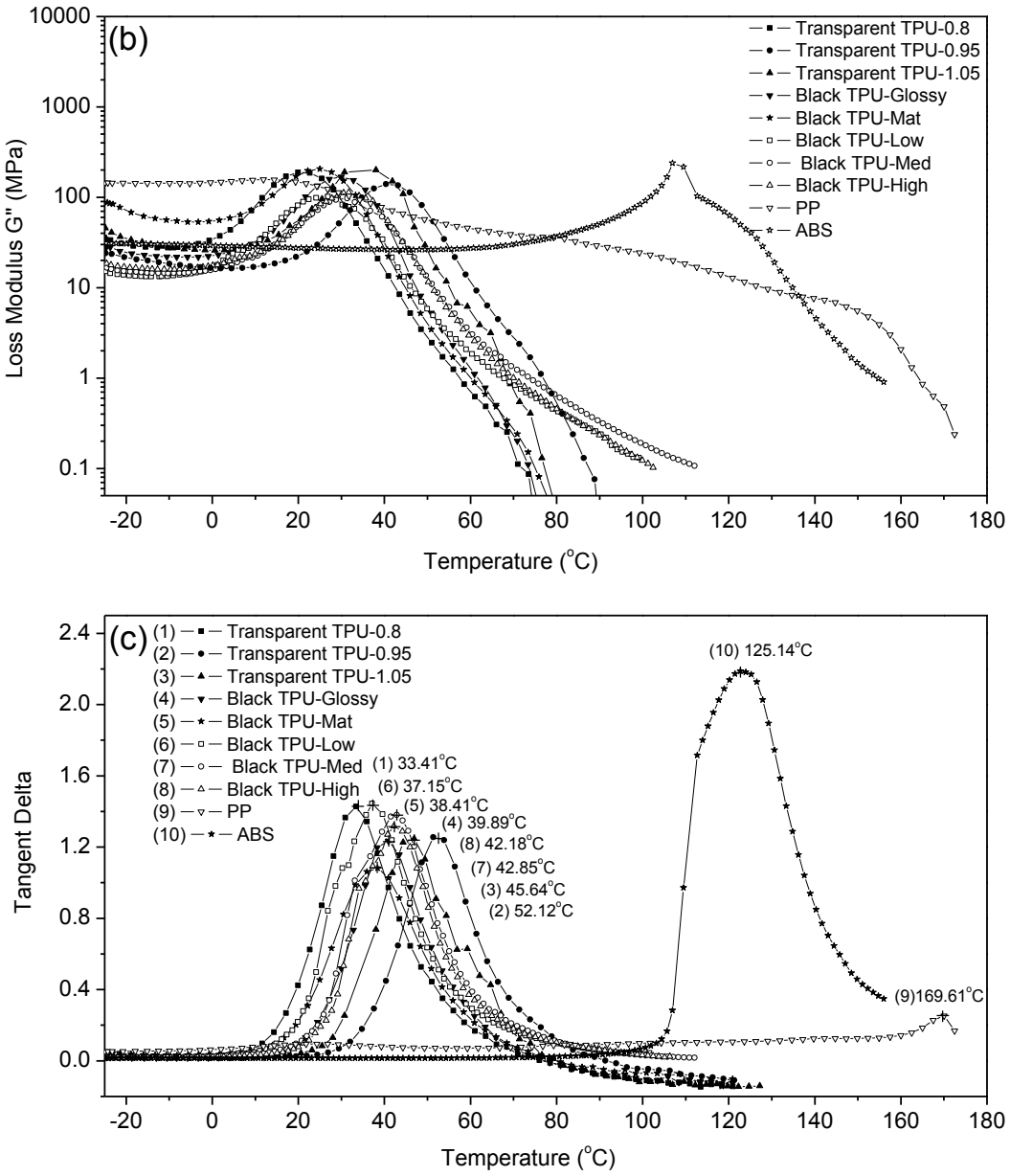

Figure 4-2 Dynamic mechanical properties of TPU films (from -25 ℃ to 120 ℃) and substrates PP and ABS (from -25 ℃ to 180 ℃)
(a) storage modulus (*G'*), **(b)** loss modulus (*G''*), **(c)** tangent delta

As shown in **Figure 4-2**, the different TPU films had similar trends of storage modulus (G'), loss modulus (G'') and tangent delta vs. temperature with a transition around 40 ℃. According to **Figure 4-2 (a)**, the storage modulus of the TPU films remained almost stable around 700-1900MPa for different TPU films in the temperature

range of -25°C to 20°C. Then G' declined exponentially from that value to a minimum value of 4MPa across the glass transition range of 20-60℃, namely T_g - 20℃ to T_g + 20℃ (Tobushi et al., 1997, Tobushi et al., 2001). Beyond 60°C, the G' value remained relatively unaltered up to 120℃.

In terms of Black TPU-Low, Med and High, it was seen that Black TPU-High exhibited the highest elastic stiffness (based on G') while Black TPU-Low was the lowest within the glass transition range. As shown in **Figure** 4-**2 (b)**, the loss modulus of the TPU films reached their peak values across the glass transition range and dropped rapidly when the temperature was over 60°C. The peak value of the tangent delta represents a mechanically defined T_g, which in this case of the TPU films was 52.12°C for Transparent TPU-0.95 as the highest one and 33.41°C for Transparent TPU-0.8 as the lowest, shown in **Figure** 4-**2 (c)**. For the Black TPU-Low, Med and High, their mechanically defined Tg were 37.15℃, 42.85℃ and 42.18℃, respectively and the glass transition behavior of the Black TPU-Med and TPU-High films appeared identical. The values of mechanically defined T_g measured by DMA testing were almost 20℃ higher than the thermally defined T_g by DSC testing. The comparison of thermal and mechanical T_g of all TPU films was shown in the **Figure 4-3** below.

As substrates, the storage modulus of the PP substrate decreased gradually from 2400MPa at 20°C to 35MPa at 150°C. Beyond 150°C, a sudden drop in the modulus value to almost 1MPa was noticed, due to melting of PP crystals (observed at 169.61°C in **Figure 4-2 (c)**) in that temperature range. The storage modulus of the ABS substrate experienced an exponential drop after remaining stable at 1100Mpa from -25°C to 100°C, with a mechanically defined T_g of 125.14°C shown in the **Figure 4-2 (c)**.

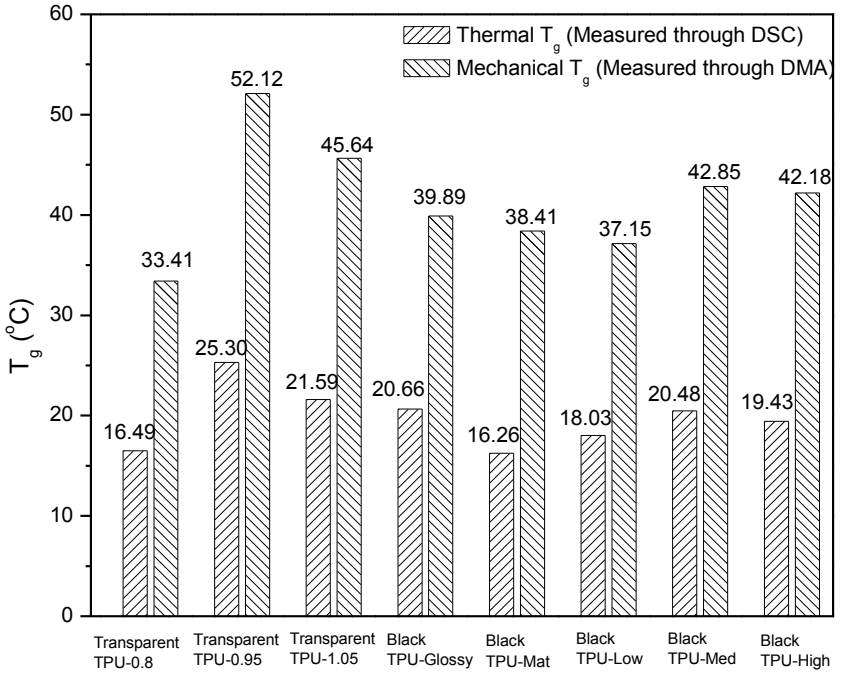

Figure 4-3 Comparison of thermally defined T_g and mechanically defined T_g of all TPU films

4.3 Tensile Test: Stress-strain Behaviour

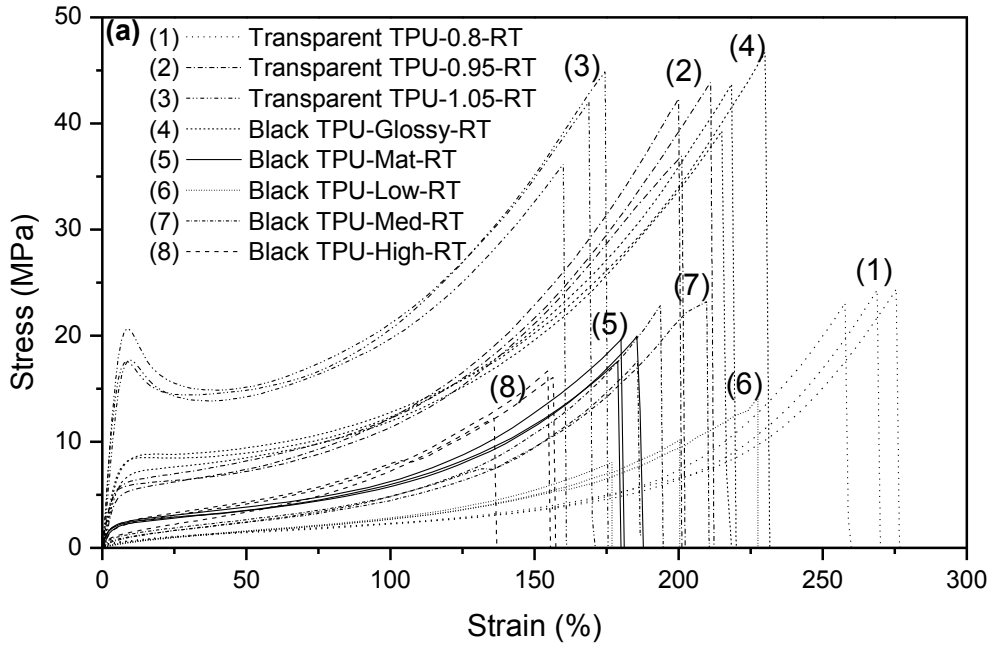

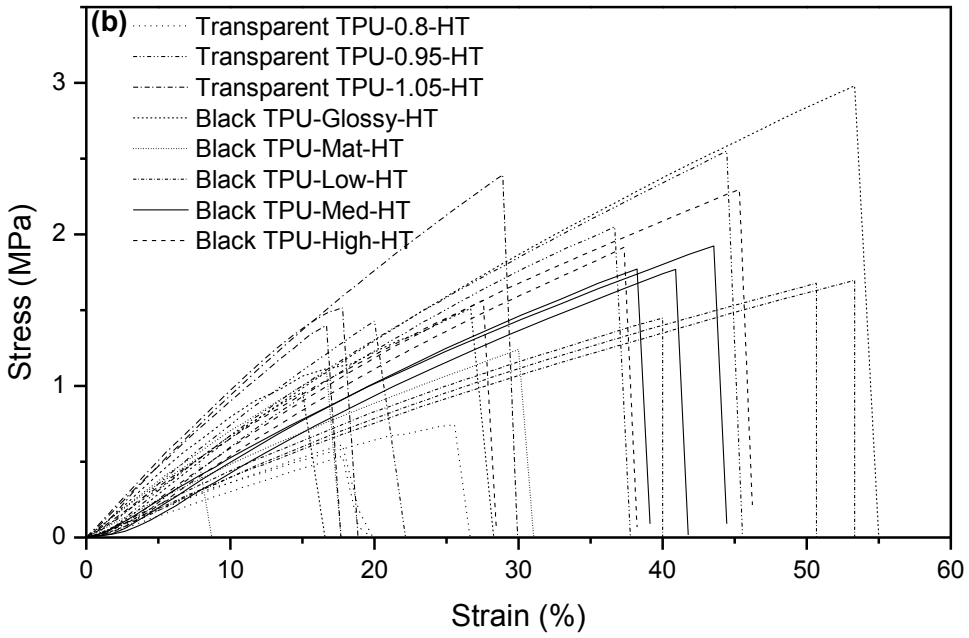

Figure 4-4 Stress-strain behaviour of all TPU films tested at **(a)** 22-23°C (RT) and **(b)** 150°C (HT)

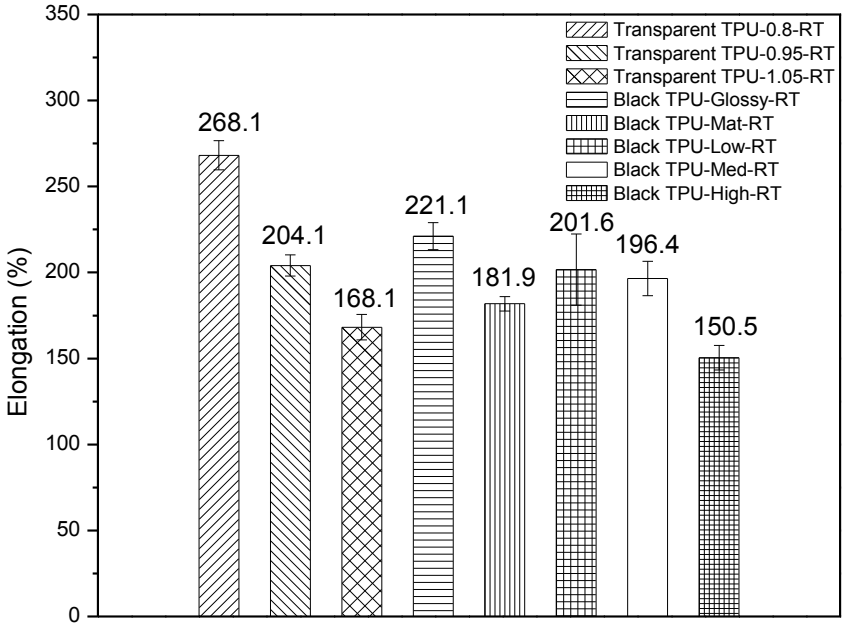

Figure 4-5 Elongation of all TPU films at 22-23°C (RT)

The stress-strain behaviour of all eight different TPU films tested at a cross head speed of 200 mm/min at 22-23°C (RT) and 150°C (HT) was illustrated in **Figure 4-4** above. The stress-strain relationship at room temperature was distinctly different from that at high temperature. At room temperature in **Figure 4-4 (a)**, the samples showed an elastomer-like stress-strain behaviour with a repeatable maximum strain-at-break in the range of 170% to 275% which decreased with the increasing monomer ratio (or increasing modulus) of TPU films (data summarized in **Figure 4-5)**. A gradual dumbbell-shaped neck spanning the entire gauge length region was observed and there was no evidence of sharp necking as usually seen in stiffer crystalline polymers. Interestingly, stress-strain behaviour of Transparent TPU-1.05 was different from those of other TPU films, with a decrease of stress occurred in the yielding stage. After the failure, the two halves of the fractured specimen recovered back to their original shape (rectangular) completely within a short span of time. These characteristics are typical for a shape recoverable elastomeric material. Among the transparent TPU films, due to relatively higher content of hard segment, the one with the highest monomer ratio, Transparent TPU-1.05, recorded the highest Young's modulus of 364.74±41.77MPa, subsequently decreased to 157.91±6.13MPa and 14.77±2.96MPa for Transparent TPU-0.95 and Transparent TPU-0.8 respectively, as shown in **Figure 4-7**. Compared to the transparent TPU films, the same trend was found for Black TPU-Low, Med and High, though with relatively lower Young's moduli of 9.12±1.35MPa, 27.74±6.11MPa and 70.24±7.79MPa respectively..

In contrast, the films tested at high temperature (150℃) showed linear stress-strain behaviour identical to a brittle specimen, seen in the stress-stain curves of **Figure**

4-4 (b). The films failed at very low stress values in the range of 0.6 to 3 MPa and the recorded strain-at-break values were also very low and unrepeatable in the range of 8-55%. The possible reasons for the TPU films failing in brittle-like fashion may be due to weakening of hydrogen bonded hard segments, or pronounced micro-phase segregation between the hard and soft segments at high temperature.

In terms of stress-strain behaviour of Black TPU-Low, TPU-Med and TPU-High tested at 45 ℃ and 65 ℃ (which were relevant to the recovery test conditions), similar linear stress-strain behaviour occurred with a relatively poor-repeatable elongation in the range of 110-230% at 45 ℃ and 85-115% at 65 ℃, as illustrated in **Figure 4-6**. As indicated in **Figure 4-7**, the Young's modulus of Black TPU-Low, TPU-Med and TPU-High experienced a sudden drop from room temperature to 45 ℃. With the temperature increasing further, the change in Young's modulus was negligible. In terms of the PP and ABS substrates, **Figure 4-8** shows it had a higher Young's modulus from room temperature to 65 ℃ and was less temperature-sensitive compared with PP.

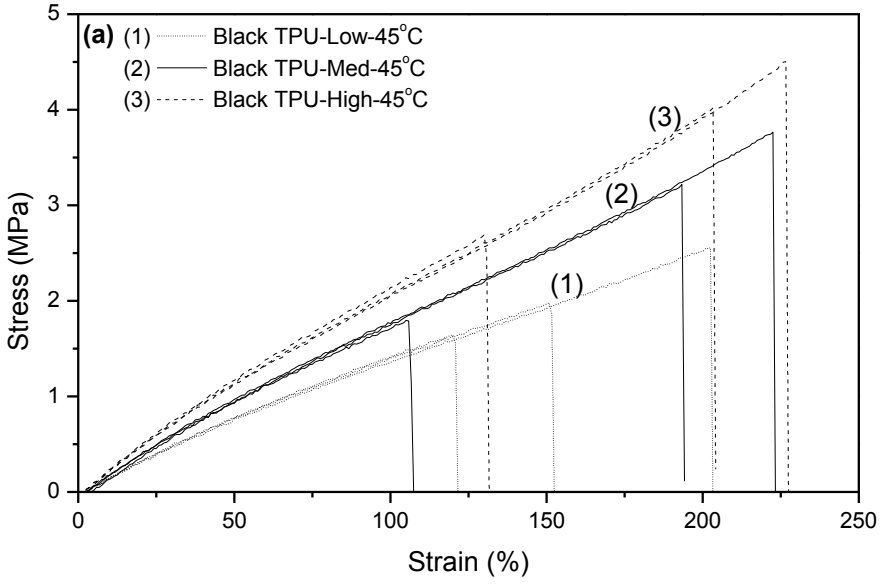

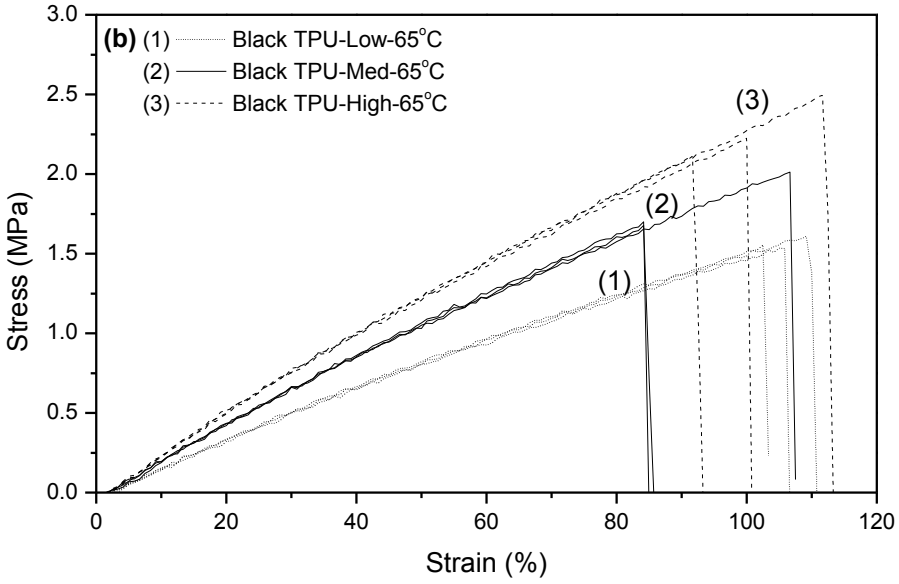

Figure 4-6 The stress-strain behaviour of Black TPU-Low, TPU-Med and TPU-High tested at **(a)** 45°C and **(b)** 65°C

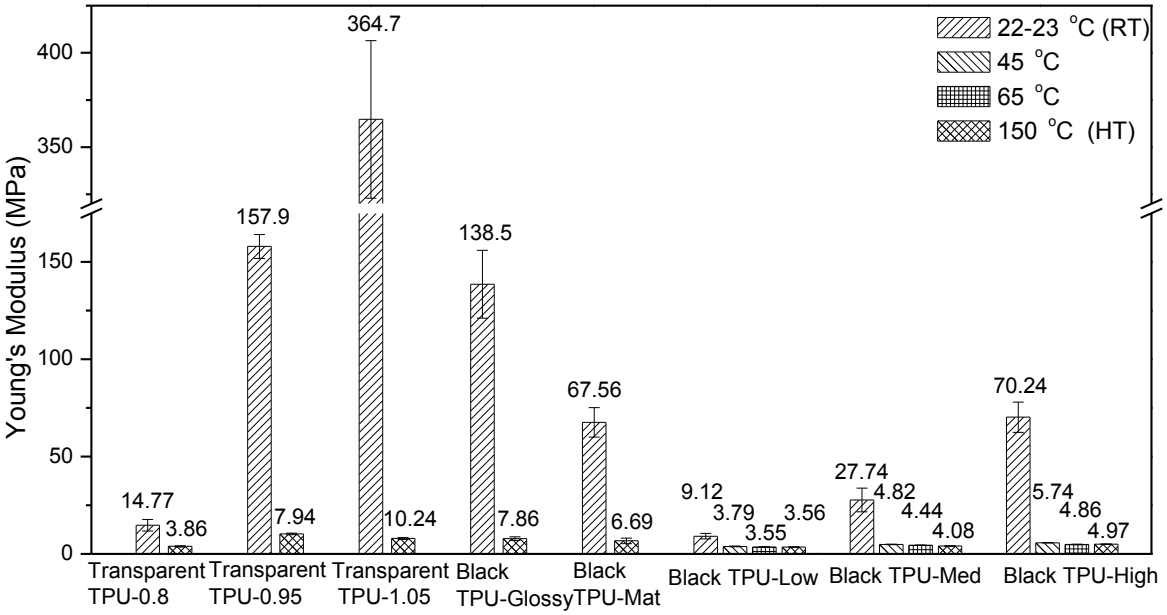

Figure 4-7 Young's modulus of TPU films at different temperatures

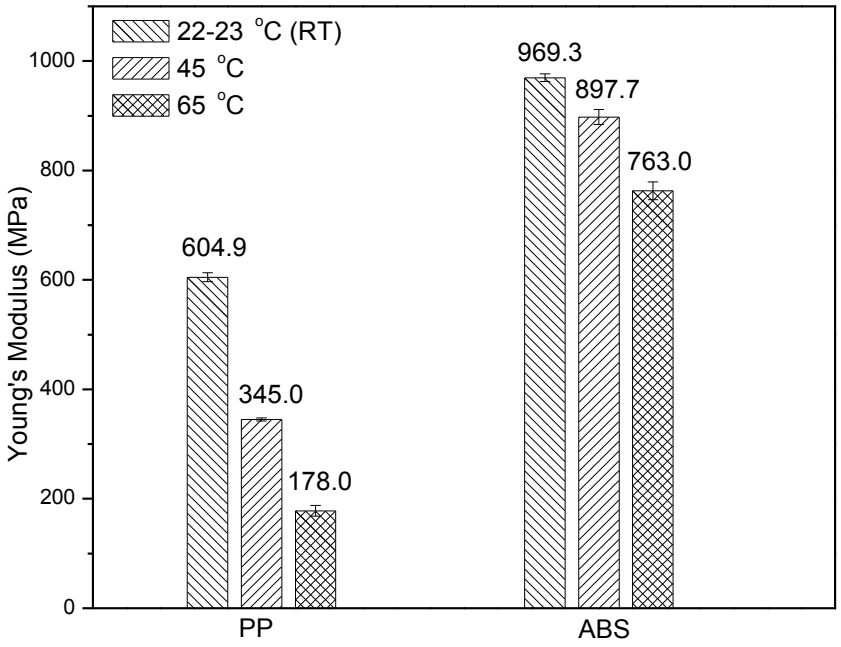

Figure 4-8 Young's modulus of PP and ABS at 22-23°C (RT), 45°C and 65°C

4.4 Relaxation Test: Stress Relaxation Behaviour

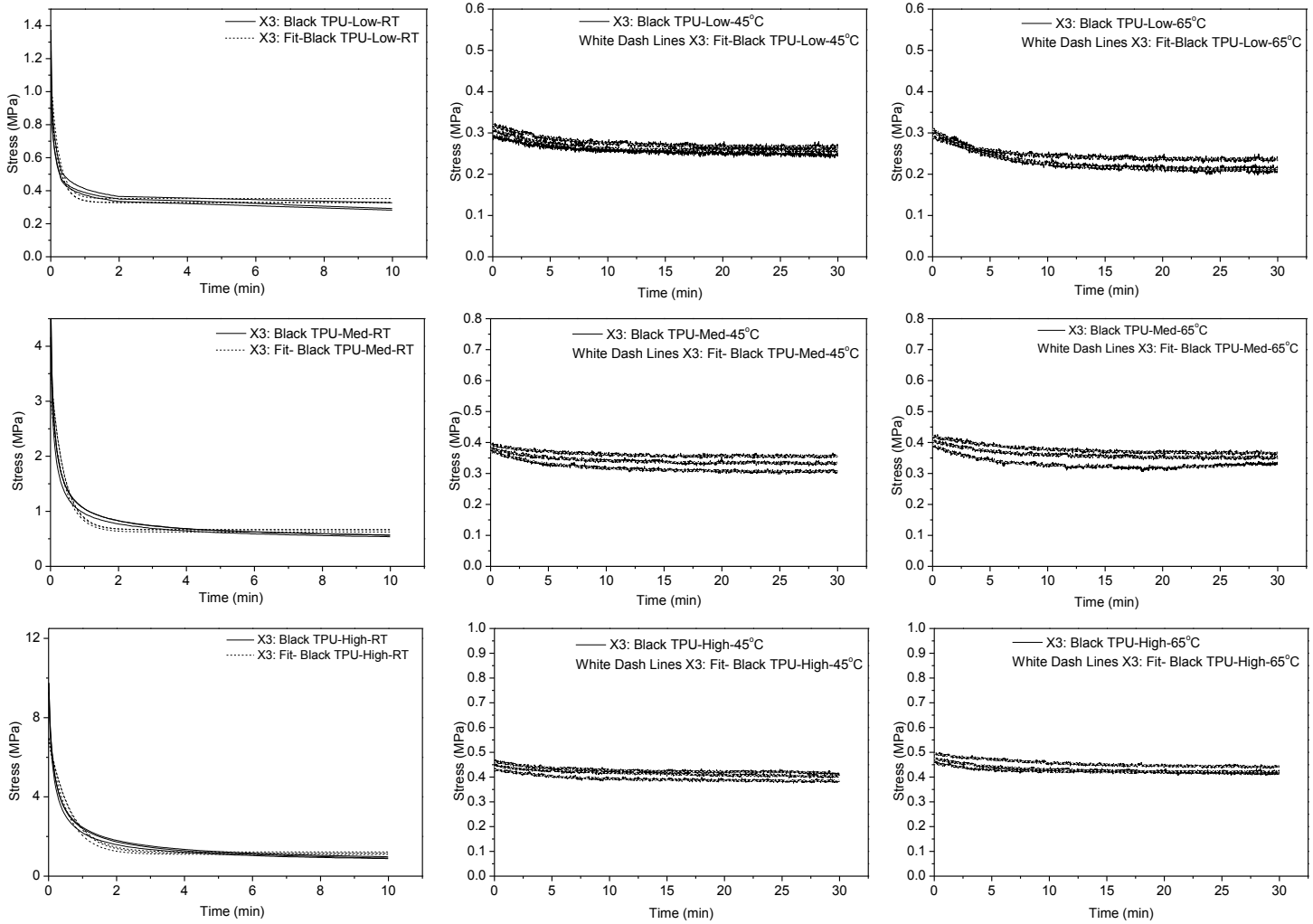

Figure 4-9 Relaxation curves of Black TPU-Low, TPU-Med and TPU-High at room temperature, 45°C and 65°C (each with three repeats)

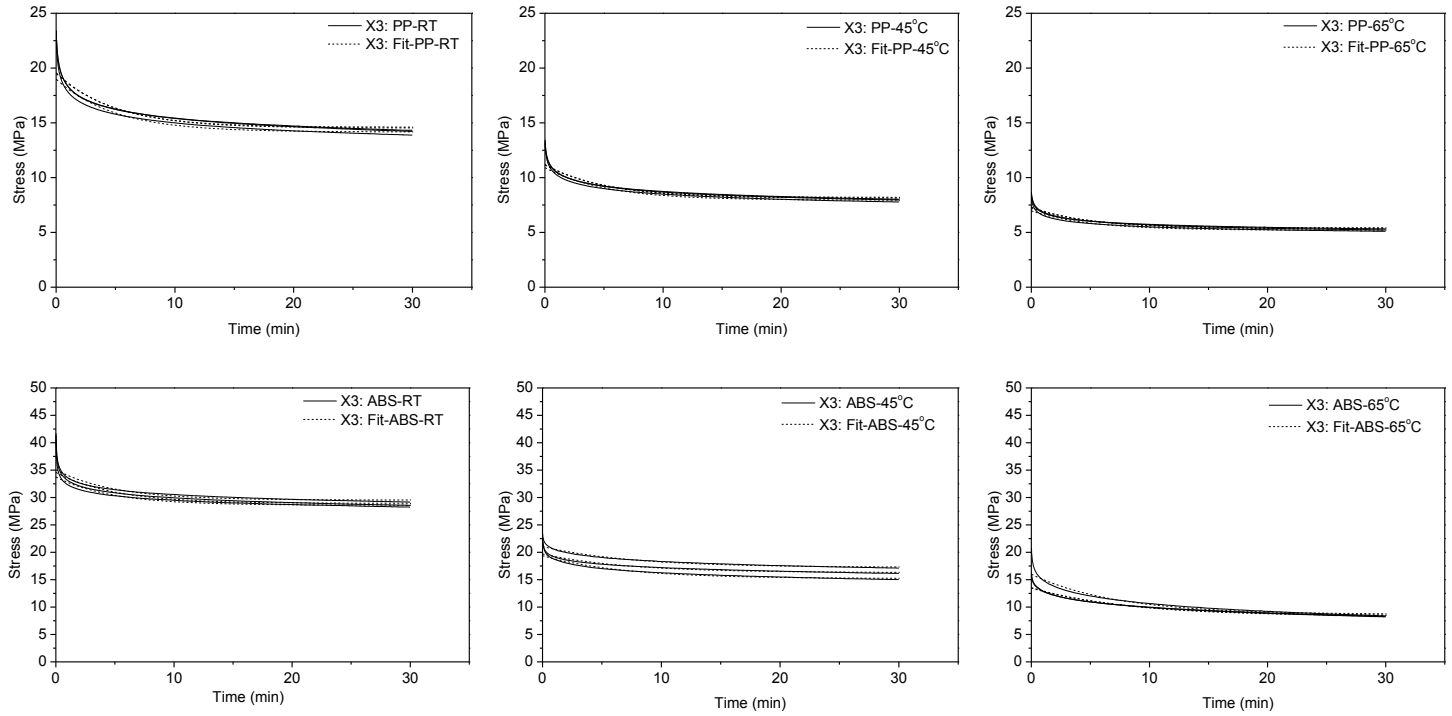

Figure 4-10 Relaxation curves of PP and ABS at room temperature, 45^{o}C and 65^{o}C (each with three repeats)

The above plots in **Figure 4-9** and **Figure 4-10** show the stress relaxation curves for three TPU films (Black TPU-Low, TPU-Med and TPU-High) and two substrates (PP and ABS) along with their fitted response to Equation **(3)**. The temperatures of the tests corresponded to the shape memory recovery study conditions. Based on the Equation **(3)**, the relaxation time τ and relaxation modulus E_{1a} of three different TPU films and two substrates were obtained and shown in the **Figures 4-11, 4-12 and 4-13**.

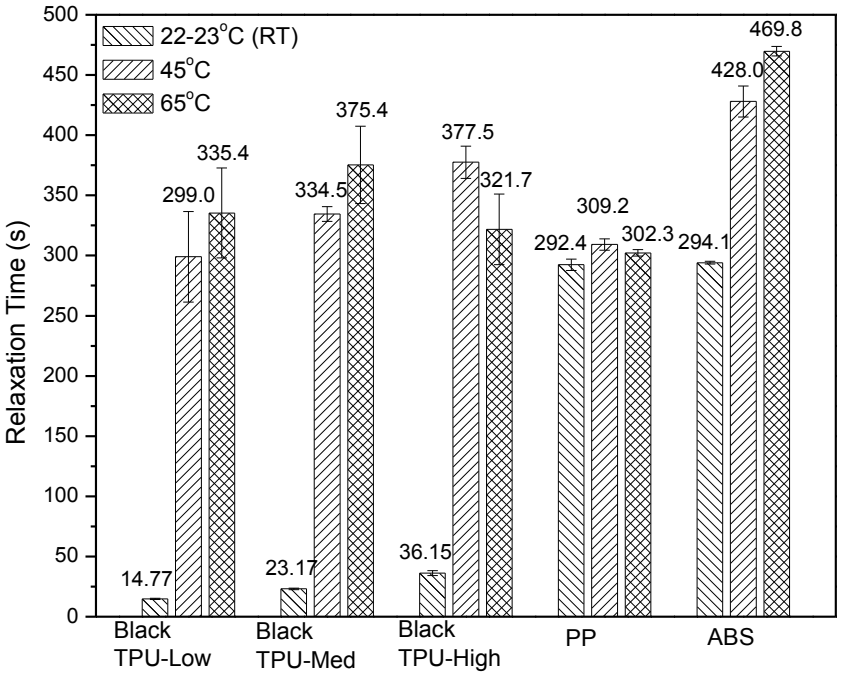

Figure 4-11 Relaxation time of Black TPU-Low, TPU-Med and TPU-High and substrates at 22-23°C (RT), 45°C and 65°C

As shown in **Figure 4-11**, the characteristic relaxation times at room temperature and 45°C increased with increasing film modulus whereas at 65°C, the Black TPU-Med exhibited the highest relaxation time. At 45°C, the relaxation times of TPU films increased significantly compared with those at room temperature, as expected with

greater viscous character. The increase in the relaxation time from 45°C to 65°C was much less than from 20°C to 45°C and even showed a decrease in time for Black TPU-High. As to the substrates, the trend in stress relaxation was consistent and followed expected behaviour. With an increase in ambient temperature from 45°C to 65°C, the relaxation time increased. For PP, the effect of temperature was minor while for ABS larger differences in relaxation times were found.

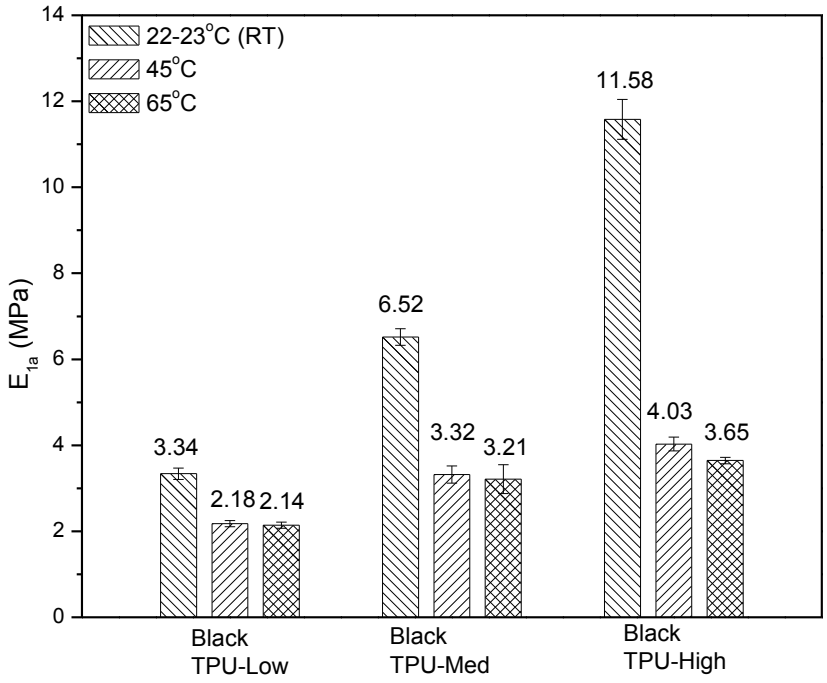

Figure 4-12 Relaxation modulus (E_{1a}) of Black TPU-Low, TPU-Med and TPU-High at 22-23°C (RT), 45°C and 65°C

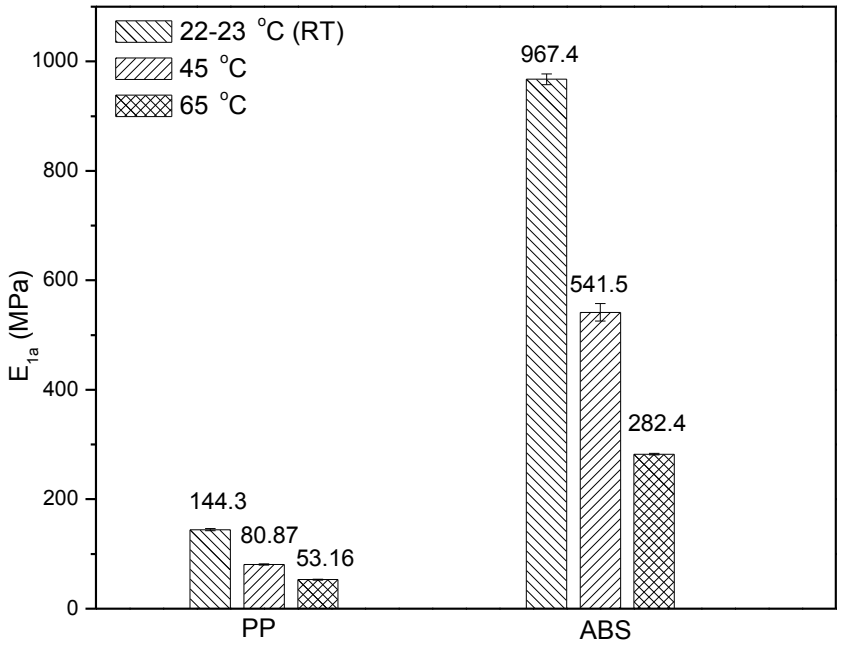

Figure 4-13 Relaxation modulus (E_{1a}) of PP and ABS at 22-23°C (RT), 45°C and 65°C

Figures 4-12 and **4-13** showed the effect of temperature on the relaxation modulus, E_{1a} of TPU films and substrates. It was shown that E_{1a} of the TPU films increased with their mechanical modulus at all three temperatures; actual mechanical moduli values at the stated temperatures are listed in **Figure 4-7**. E_{1a} of TPU films and substrates decreased with temperature notably from room temperature to 45°C. With a further increase in temperature, E_{1a} of both substrates further decreased while that of TPU films showed little change. These findings will be important to discussing results from the recovery study in the following chapter.

Chapter 5 Modeling

5.1 Modeling Description

In order to have a better understanding of the data from experiments, a model was developed to describe recovery behavior of the formed TPU based laminates based on the mechanics analysis of substrate layers during the recovery.

During the recovery process, two assumptions were made: (1) the arc length of laminates was constant; and (2) formed laminate recovered along the path of a circular arc with a changing central angle. As the recovery process of formed laminates was relatively slow, the substrate layer was assumed being in a dynamic balance- the restorative bending moment from TPU layer towards the direction of recovery is balanced with the retarding bending moment from substrate itself due to its curvature (thermal expansion effects of the polymers are ignored in this model). It is assumed that the adhesive is strong enough that there is no exfoliation or delamination between TPU and substrate layers during the recovery process. However, since the adhesive is relatively thick (0.125mm) and low in its shear storage moduli (below 0.025MPa from 20^{o}C to 65^{o}C as shown in **Figure 5-1**, which was measured by ARES Rheometer) with respect to the TPU layer (0.2mm thickness, above 5MPa in storage moduli from 20^{o}C to 65^{o}C from DMA data) and substrate layer, the influence of the adhesive layer on the dynamic balance of bending moments on the substrate layer cannot be ignored. Owing to possible shear deformation in the adhesive, that layer is assumed to consume/dissipate part of the recovery stresses from TPU layers. Therefore, only a portion of the recovery

stresses can be transferred onto substrate layer for recovery (*TR* (%) as a stress transfer ratio in this model).

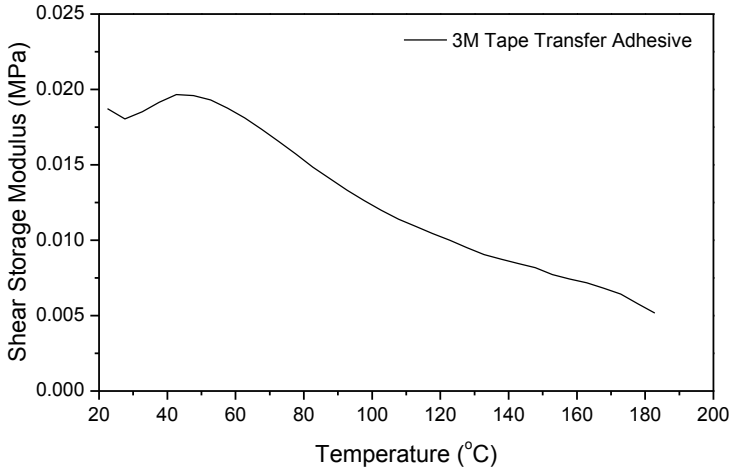

Figure 5-1 Shear storage moduli of 3M tape transfer adhesive vs. temperature

Due to the large out-of-plane deformation for the laminate in the forming process, the width and thickness of both TPU and substrate layers were changed by following Equation **(5-1)** (Krevelen and Nijenhuis, 2010).

$$\Delta d = -d \cdot [1-(1+\frac{\Delta L}{L_0})^{-\nu}] \qquad \textbf{(5-1)}$$

where d is the original value of width or thickness of layers, [units of m]; Δd is the change of the width or thickness [units of m]; ν is the Poisson's ratio of TPU films or substrates; L_0 is the original length of laminate before forming [units of m]; ΔL is the change of length after forming [units of m]. The value is negative because it decreases with increase of length.

In this model, a standard linear viscoelastic (SLV) constitutive model (Leng and Du, 2012) was used for the TPU layer and the Kelvin–Voigt model (Leng and Du, 2012)

was used for each type of substrate layer. As shown in **Figure 5-2** below, the substrate layer is suffering a force at its periphery from the TPU layer (*F(θ, t)*) during the whole process of recovery. Based on Newton's third law, *F(θ, t)* is equal to the recovery force of TPU layer which can be

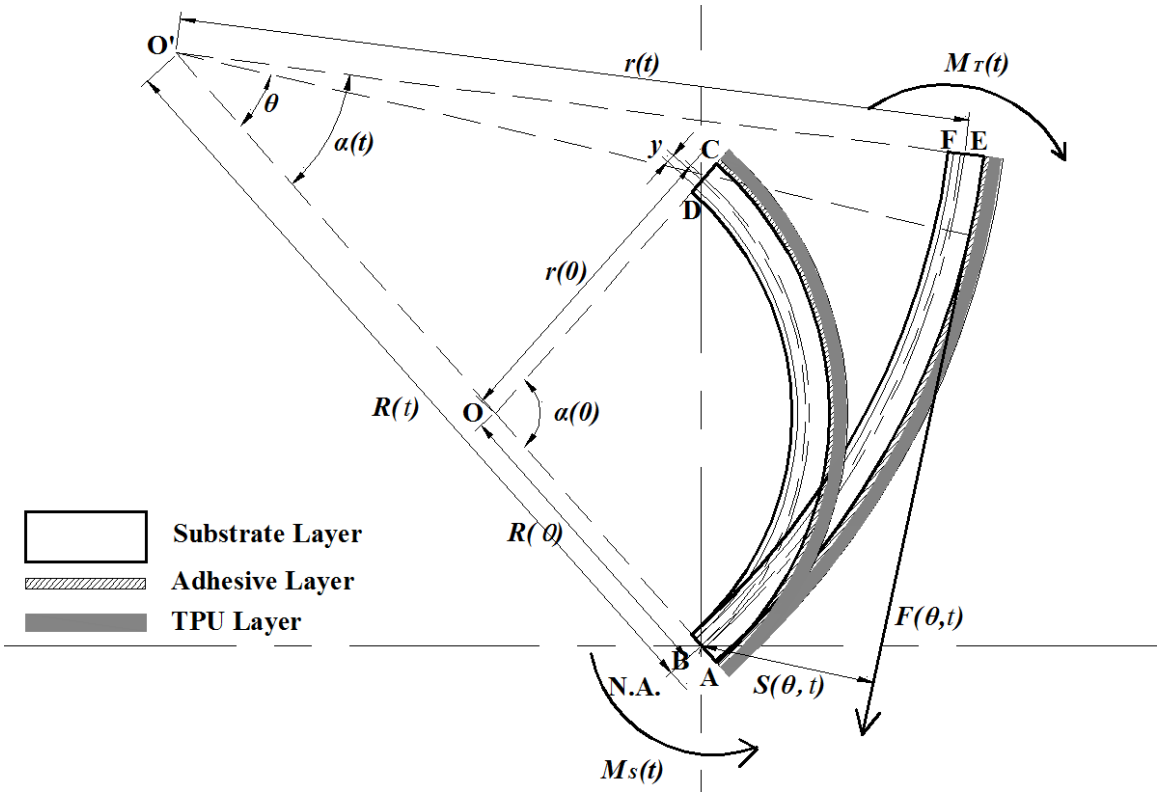

Figure 5-2 Schematic diagram of mechanics analysis for TPU based laminate during recovery (Top view)

obtained from the SLV model (Leng and Du, 2012) ($\dot{\varepsilon}_1$ is 0 as ε_1 is kept constant during recovery). The expressions of *F(θ, t)* are shown in Equation **(5-2)** and **(5-3)**.

$$F(\theta,t) = TR \times A_T \times \sigma_1 \tag{5-2}$$

$$\dot{\sigma}_1 + \frac{\sigma_1}{\lambda_1} - \frac{E_{1a}\varepsilon_1}{\lambda_1} = 0 \tag{5-3}$$

where *TR* is the stress transfer ratio through the adhesive layer; A_T is the area of the cross-section of TPU layer after forming [units of m^2]; σ_1 and ε_1 denote recovery stress (N/m^2) and strain (%) of TPU layer, respectively; E_{1a} and $\lambda_1 = \frac{\eta_1}{E_{1b}}$ present Young's modulus (Pa) of equilibrium response and relaxation time (s) of TPU layer in SLV model, respectively. The dot denotes time derivative.

As we can see in the **Figure 5-2**, the restorative bending moment ($M_T(\theta, t)$) generated by $F(\theta, t)$ at central angle of θ and time t is expressed in Equation **(5-4)** and **(5-5)**.

$$M_T(\theta,t) = F(t) \times S(\theta,t) \quad \textbf{(5-4)}$$

$$S(\theta,t) = r(t) + \frac{1}{2}H_S - R(t)\cos(\theta) \quad \textbf{(5-5)}$$

where $S(\theta, t)$ is the arm of $F(\theta, t)$ at central angle of θ and time t [units of m]; $r(t)$ is the distance from the center of curvature *O'* to the centroid of the cross section of substrate layer at time *t*, [units of m]; *R(t)* is the corresponding radius of substrate layer at time *t*, which is the distance from the center of curvature *O'* to the neutral axis (N.A.) of the cross section of substrate layer [units of m]; H_S is the thickness of substrate layer after forming [units of m]. In a curved member, the neutral axis of a transverse section does not pass through the centroid of that section. For cross-sectional shape of rectangle, the relationship between *R(t)* and $r(t)$ is as follows (Beer et al., 2009).

$$R(t) = \frac{H_S}{\ln \dfrac{r(t) + \dfrac{H_S}{2}}{r(t) - \dfrac{H_S}{2}}} \quad \textbf{(5-6)}$$

The relationship between the overall bending moment at time t ($M_T(t)$) and $R(t)$ can be calculated through integration of $M_T(\theta, t)$ by θ along the laminate, which is shown in the Equation **(5-7)** and **(5-8)**.

$$M_T(t) = \int_0^{\alpha(t)} F(t) \times S(\theta, t) d\theta = F(t) \times \left\{ \alpha(t) \times \left[r(t) + \frac{1}{2} H_S \right] - R(t) \sin \alpha(t) \right\} \quad \textbf{(5-7)}$$

$$\alpha(t) = \frac{L_S}{R(t)} \quad \textbf{(5-8)}$$

where $\alpha(t)$ is the central angle of formed laminate at time t; L_S is the length neutral axis of substrate after forming [units of m].

$M_S(t)$ represents the retarding bending moment generated by the substrate layer due to its corresponding curvature at time t. Based on the assumption that the substrate layer was in dynamic balance, $M_T(t)$ and $M_S(t)$ are equal and opposite, coupled across a plane of symmetry within the laminate (shown in **Figure 5-2**), namely

$$M_T(t) = M_S(t) \quad \textbf{(5-9)}$$

The recovery process on a substrate layer is assumed to be purely bending. The intersection of its neutral axis has been represented in **Figure 5-2** by the arc AC of radius of $R(0)$ at t=0 and the arc of AE of radius of $R(t)$ at time t. Denoting by $\alpha(0)$ and $\alpha(t)$ these central angles corresponded to arc lengths AC and AE, respectively. The fact that the length of the neutral axis remained constant can be expressed as

$$R(0)\alpha(0) = R(t)\alpha(t) = L_S \tag{5-10}$$

where $\alpha(0)$ is the initial central angle of the substrate after forming, which can be expressed as

$$\alpha(0) = 2\arccos(\frac{R_m - h}{R_m}) \tag{5-11}$$

and h is the draw value [units of m]; R_m is the radius of the male mold [units of m].

Considering the arc of circle BF located at a distance y above the neutral axis, at time t, the deformation of BF can be expressed as

$$\delta = \alpha(t)[R(t) - y] - \alpha(0)[R(0) - y] = y[\alpha(0) - \alpha(t)] \tag{5-12}$$

The normal strain of substrate layer ε_2 (%) in the elements of BF is obtained by dividing the deformation δ by its initial length (arc BD), $\alpha(0)[R(0) - y]$,

$$\varepsilon_2 = \frac{y[\alpha(0) - \alpha(t)]}{\alpha(0)[R(0) - y]} \tag{5-13}$$

$$\dot{\varepsilon}_2 = \frac{-y}{\alpha(0)[R(0) - y]} \frac{d[\alpha(t)]}{dt} \tag{5-14}$$

The normal stress in the substrate layer σ_2 (N/m^2) can be obtained from the Kelvin–Voigt model (Leng and Du, 2012),

$$\sigma_2 = E_2\varepsilon_2 + \eta_2\dot{\varepsilon}_2 \tag{5-15}$$

Based on the theory of pure bending of curved members (Beer et al., 2009), $M_S(t)$ can be expressed as

$$M_S(t) = \int y \times \sigma_2 dA \tag{5-16}$$

Substituting for σ_2 from Equation **(5-10)-(5-15)** to Equation **(5-16),** integrating and solving, got

$$M_S(t) = \frac{A_S e E_2}{\alpha(0)}[\alpha(0) - \alpha(t)] - \frac{A_S e \eta_2}{\alpha(0)} \frac{d[\alpha(t)]}{dt} \quad \textbf{(5-17)}$$

where A_S is the area of the cross-section of substrate layer after forming [units of m^2]; E_2 and η_2 present Young's modulus (Pa) and viscosity (Pa·s) of the substrate layer in the Kelvin–Voigt model, respectively; e is the distance between the neutral surface and centroid of a transverse section of the curved substrate layer at time t, namely $r(t)$ - $R(t)$ [units of m]; The dot denotes time derivative.

Combining Equations **(5-7)**, **(5-9)** and **(5-17)**, got

$$\frac{dR_a(t)}{dt} = -\frac{E_2 R_a(t)}{\eta_2} + \frac{F(t)}{A_S e \eta_2}\left[\alpha(0)[1-R_a(t)]\left\{\frac{H_S}{\exp\{\frac{H_S[1-R_a(t)]}{R(0)}\}-1} + H_S\right\} - \frac{R(0)}{1-R_a(t)}\sin\{\alpha(0)[1-R_a(t)]\}\right] \quad \textbf{(5-18)}$$

where $R_a(t) = \frac{\alpha(0)-\alpha(t)}{\alpha(0)} \times 100\%$ presents the angle recovery ratio for the sake of measuring the degree of recovery of the laminate at time t, units of %. Therefore, based on the above Equation **(5-18)**, the relationship between $R_a(t)$ and t can calculated through MATLAB, the code of the model is provided in Appendix. All values of constant parameters in above equations are listed in **Table 5-1**.

Table 5-1 Values of constant parameters in above equations

Stress transfer ratio through the adhesive layer, TR (%)	3
Radius of male mold, R_m (m)	2.5×10^{-2}
Original thickness of substrate layer, H_{S0} (m)	0.5×10^{-3}

Original thickness of TPU layer, H_{T0} (m)	0.2×10^{-3}
Original width of laminate, w (m)	1.27×10^{-2}
Possion's ratio of TPU, ν_T	0.50
Possion's ratio of PP, ν_P	0.42
Possion's ratio of ABS, ν_A	0.35

5.2 Dependence of Coefficients on Temperature

It is assumed that the temperature of laminates is changing in an exponential manner. The equation expressed by an exponential function as Equation **(5-19)** is shown as dashed lines in **Figure 5-3** below.

$$T = T_{\text{Recovery}} - (T_{\text{Recovery}} - 273)\exp(-kt) \qquad \textbf{(5-19)}$$

where T_{Recovery} is the recovery temperature which was either 288K (15^{o}C), 318K (45^{o}C) and 338K (65^{o}C). k is a constant representing the overall heat transfer coefficient of laminates [units of K/s]. Based on the comparison below between real and fitted temperature of laminate vs. time during recovery as shown in **Figure 5-3**, k was selected as 0.015 K/s.

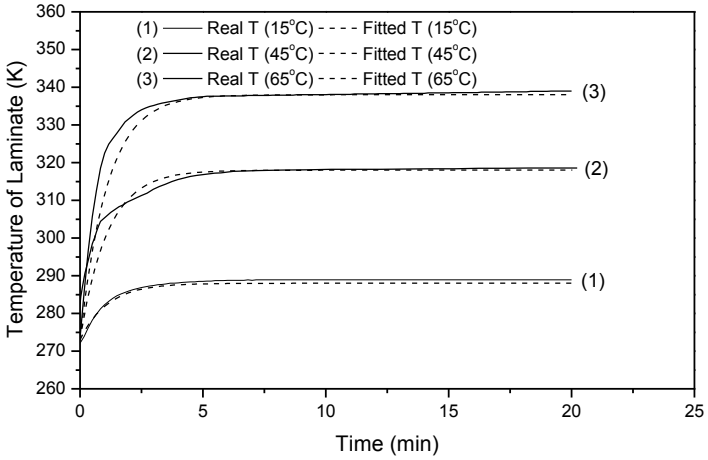

Figure 5-3 Comparison between real and fitted temperature of laminate vs. time during recovery with k=0.015 K/s

In polymers, E, η and λ are temperature-dependent parameters, especially above their glass transition region where these properties vary remarkably (Liu et al., 2006). In this model, temperature-dependent coefficients involved in above equations need to be considered (though as already noted, thermal expansion was neglected).

In terms of the TPU film, based on the work of Tobushi (Tobushi et al., 2001), E changes around T_g but keeps almost constant far above or below the glass transition region. The relationship between log E and T_g/T is expressed by a straight line in the glass transition region (T_g-$T_w \leq T_g \leq T_g$+T_w, T_w=25K), which is expressed in Equation **(5-20)**.

$$\log E - \log E_g = a\left(\frac{T_g}{T} - 1\right) \qquad \textbf{(5-20)}$$

Therefore E is

$$E = E_g \exp\left\{a\left(\frac{T_g}{T} - 1\right)\right\} \qquad \textbf{(5-21)}$$

In Equation **(5-21),** E_g is the value of E at $T=T_g$ and a is a constant representing slope of the straight line. The variation of η and λ around the glass transition was assumed similar manner to E. Thus, it was assumed that E, η and λ are expressed through an exponential function of T similar to Equation **(5-21)** (Tobushi et al., 2001). E, η and λ in SLV model of TPU films are expressed as follows:

$$E_{1a} = E_{ag} \exp\left\{a\left(\frac{T_g}{T} - 1\right)\right\} \qquad \textbf{(5-22)}$$

$$E_{1b} = E_{bg} \exp\left\{b\left(\frac{T_g}{T} - 1\right)\right\} \qquad \textbf{(5-23)}$$

$$\eta_1 = \eta_{1g} \exp\left\{c\left(\frac{T_g}{T} - 1\right)\right\} \qquad \textbf{(5-24)}$$

$$\lambda_1 = \frac{\eta_1}{E_{1b}} = \frac{\eta_{1g}}{E_{bg}} \exp\left\{(c-b)\left(\frac{T_g}{T} - 1\right)\right\} = \lambda_{1g} \exp\left\{(c-b)\left(\frac{T_g}{T} - 1\right)\right\} \qquad \textbf{(5-25)}$$

where E_{ag}, E_{bg}, η_{1g}, and λ_{1g} are the value of E_{1a}, E_{1b}, η_1 and λ_1 at $T=T_g$ (293K, 20^{o}C) and a, b and c are constants representing slopes of each straight line on semi-logarithmic diagrams. In this model, E_{ag}, λ_{1g}, a, b and c are obtained based on the fitting of experimental data as shown in **Figure 5-4** and **Figure 5-5**. All values of coefficients of the TPU films are listed in **Table 5-2**.

Table 5-2 Values of coefficients of TPU films

TPU films	E_{1g} (MPa)	λ_{1g} (s)	*a*	*c-b*
TPU-Low/45°C	4.409	14.77	10.66	-38.26
TPU-Med/ 45°C	9.322	23.17	15.33	-33.96
TPU-High/ 45°C	16.65	36.15	20.27	-29.84
TPU-Low/65°C	4.762	20.23	7.857	-24.50
TPU-Med/ 65°C	10.38	30.56	11.41	-21.84
TPU-High/ 65°C	18.98	48.07	15.52	-17.36

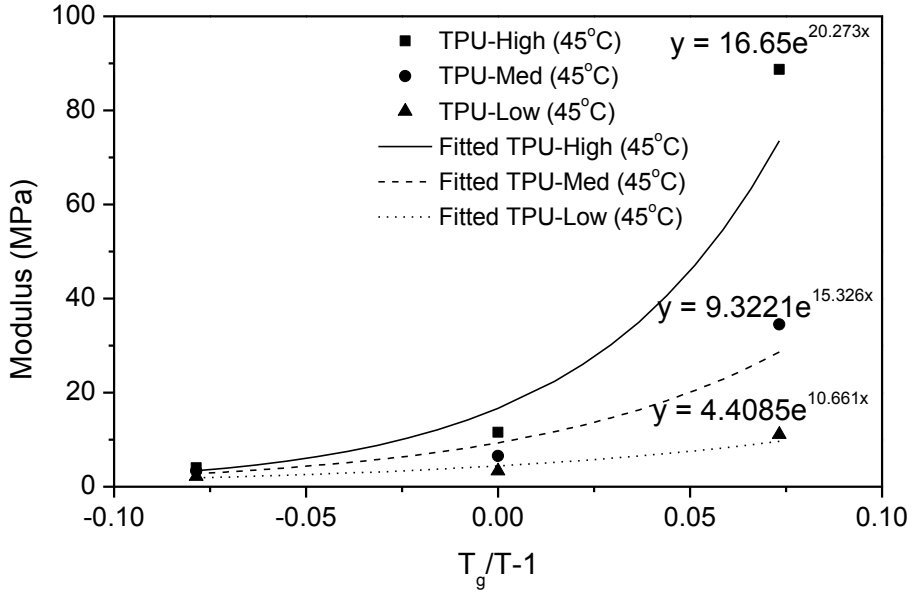

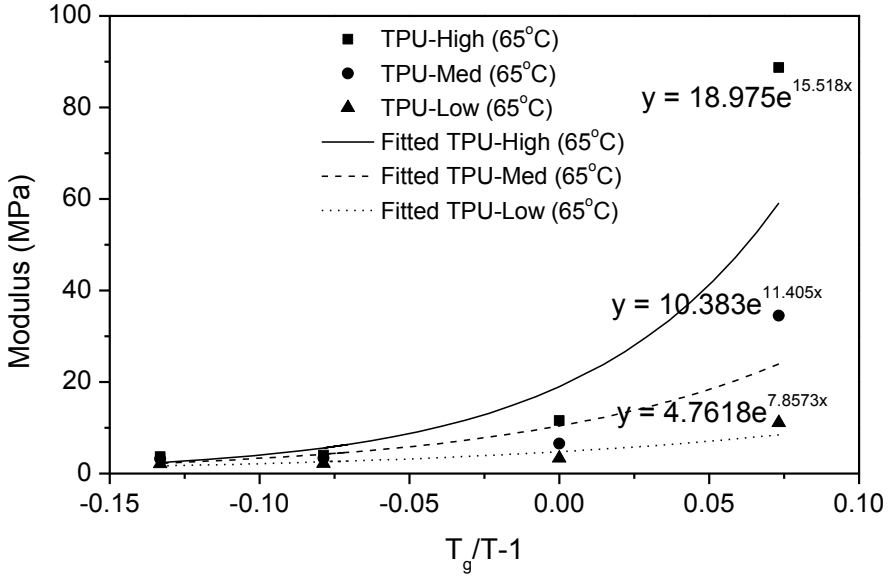

Figure 5-4 Fitting on experimental data of TPU's modulus through an exponential function of T at the recovery temperature of 45°C and 65°C (using relaxation modulus of those TPU films instead at temperature above 20°C, i.e. $T_g/T-1<0$)

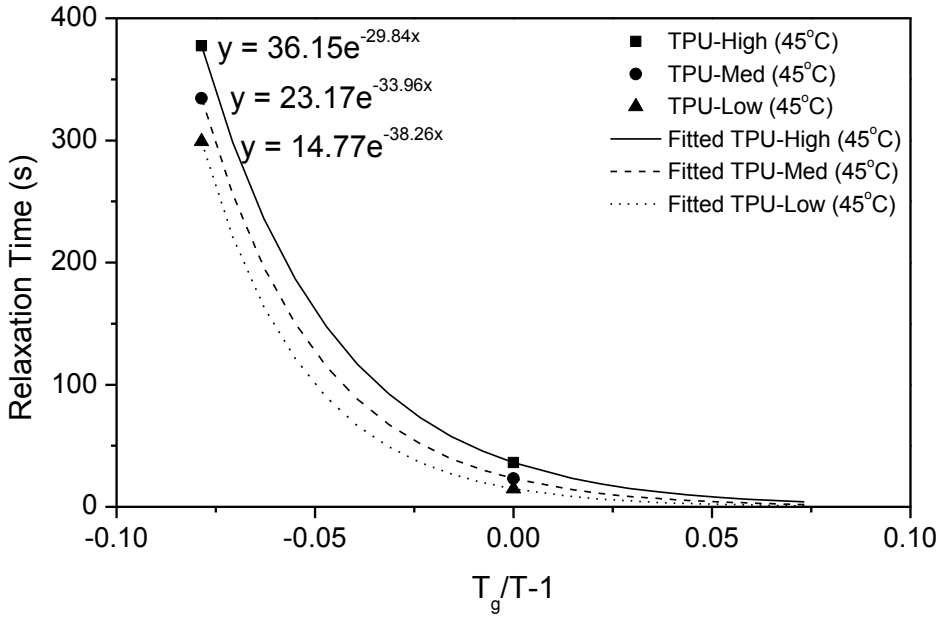

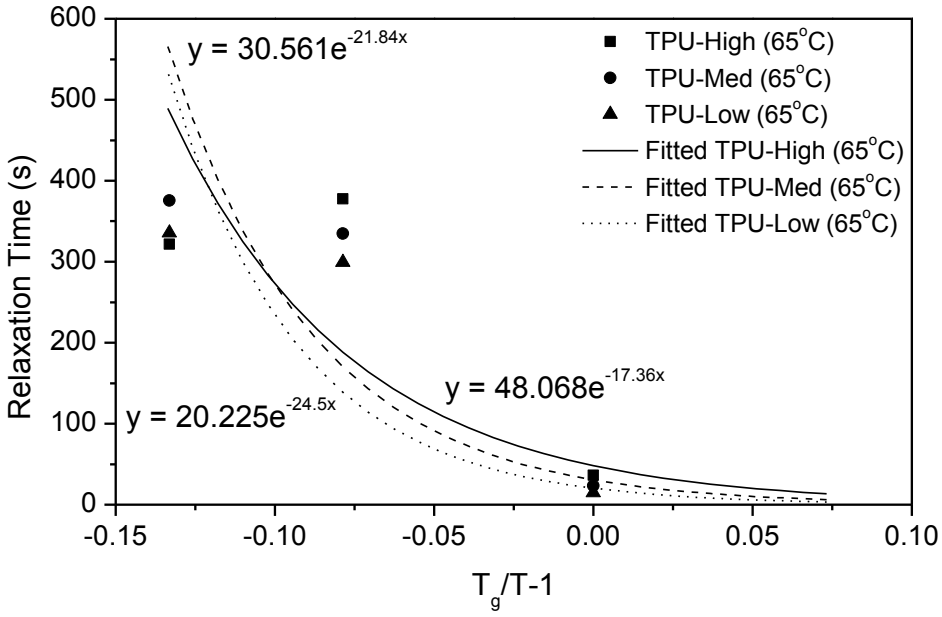

Figure 5-5 Fitting on experimental data of TPU's relaxation time through an exponential function of T at the recovery temperature of 45°C and 65°C

Among the substrates, their T_g (PP's T_g is below 0°C and ABS's T_g is around 125°C as shown in DMA test in earlier Figure **4-2**) are out of the range of environmental temperature change used in the recovery test (0~65°C). However, based on the trend of experimental data of their modulus, it is also assumed that E_2 and η_2 in the Kelvin–Voigt model for the substrates changed through an exponential function of T similar to Equation **(5-21).**

$$E_2 = E_{2g} \exp\left\{ f\left(\frac{T_g}{T} - 1\right) \right\} \quad \textbf{(5-23)}$$

$$\eta_2 = \eta_{2g} \exp\left\{ g\left(\frac{T_g}{T} - 1\right) \right\} \quad \textbf{(5-24)}$$

where E_{2g} and f are obtained based on the fitting of experimental data as shown in **Figure 5-6**. The viscosity values (η_{2g}) of PP and ABS in the temperature range of 0~65^{o}C are extremely high as the environmental temperatures are far below from their processing temperatures(Robert and Nielsen, 1993). The order of magnitude for those viscosity values was referenced from Ghosh's work (Ghosh and Srinivasa, 2013). All values of the coefficients of PP and ABS are listed in **Table 5-3**.

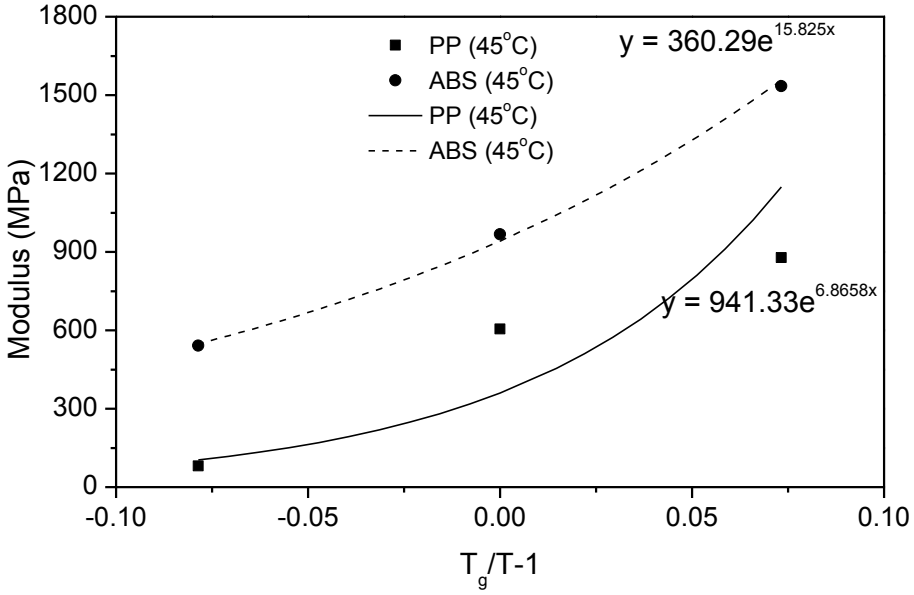

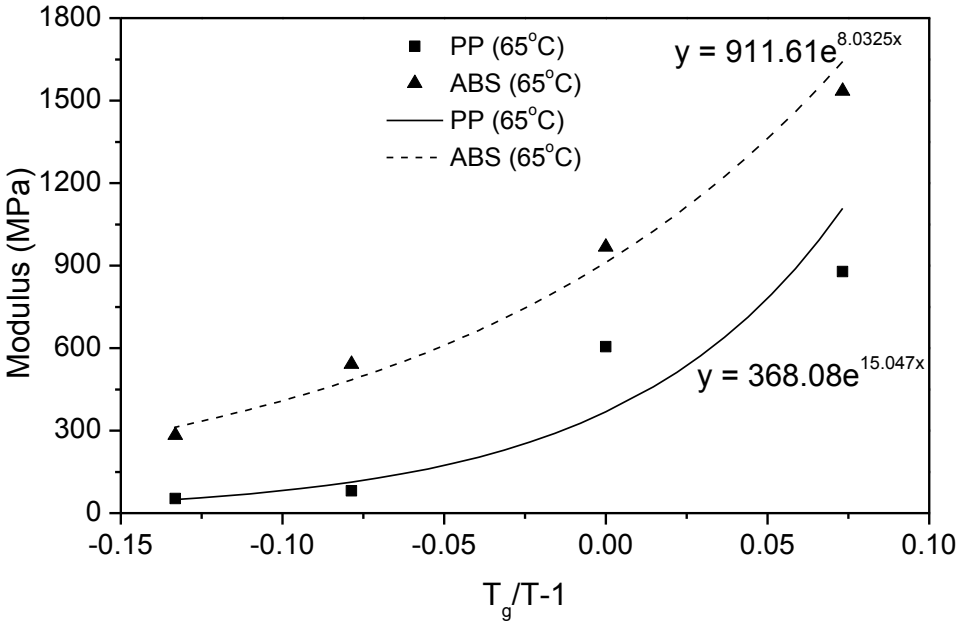

Figure 5-6 Fitting on experimental data of substrates' modulus through an exponential function of T at the recovery temperature of 45°C and 65°C (using relaxation modulus of PP and ABS instead at temperature above 20°C, i.e. $T_g/T-1<0$)

Table 5-3 Values of coefficients of substrates

Substrates	E_{2g} (MPa)	η_{2g} (GPa s)	f	g
PP/45°C	360.3	1×10^7	15.83	115
ABS/ 45°C	941.3	1.5×10^7	6.865	115
PP/ 65°C	368.1	0.8×10^7	15.04	70
ABS/65°C	911.6	1.5×10^7	8.033	70

Chapter 6 Results and Discussion

6.1 Influence of SMP's Properties on Recovery Behaviour of Laminate

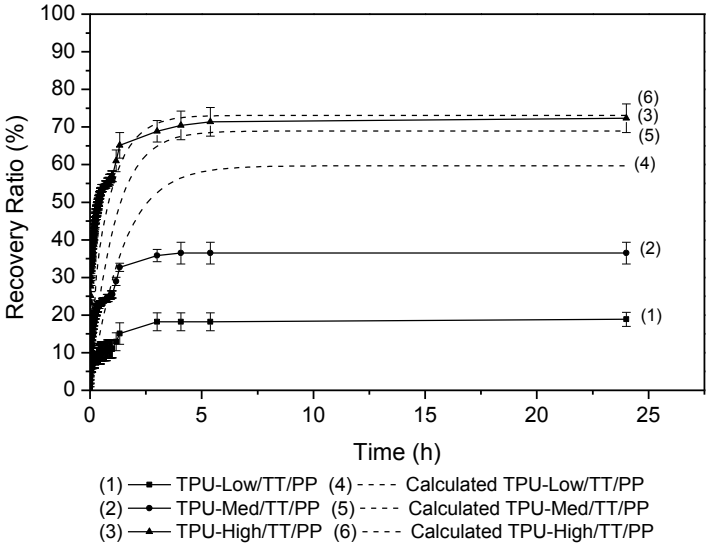

Figure 6-1 Angle recovery ratio curves (form both experiment and model) of laminates with different TPU films/ 3M tape transfer adhesive/ PP at an environmental temperature of 45°C. Error bars represent the standard deviation based on at least five repeats, same as the data of other experimental angle recovery ratio curves below

Table 6-1 Final angle recovery ratio after 24h ($R_{a,\,final}$, %) and recovery rates (%/h) of laminates (form both experiment and model) with different TPU films/ 3M tape transfer adhesive/ PP at an environmental temperature of 45°C

Laminates	Final angle recovery ratio after 24h ($R_{a,\,final}$, %)	Recovery rates (%/h)	$R_{a,\,final}$ From model (%)	Recovery rates From model (%/h)
TPU-Low/TT/PP	18.87±1.89	83.01	59.69	18.30
TPU-Med/TT/PP	36.48 ±2.89	173.58	68.94	38.63
TPU-High/TT/PP	72.33±3.81	426.42	73.10	82.31

As is illustrated in the **Figure 6-1** and **Table 6-1** below, the experimental final angle recovery ratios and recovery rates (the secant slope of the angle recovery ratio curve for the first 5 minutes of recovery, %/h) of formed TPU based laminates increased with the Young's modulus of the TPU films from low to high. After three hours, the experimental angle recovery ratios were almost stable for all three laminates with differing TPU film. By five hours, all memory-induced stresses ceased to produce further recovery at this temperature. The final angle recovery ratio of formed laminates with TPU of Young's modulus from low to high were 18.87±1.89% (corresponding to a final central angle as $86.0^{o}\pm2.0^{o}$), 36.48 ±2.89% ($67.0^{o}\pm3.1^{o}$) and 72.33±3.81% ($29.0^{o}\pm4.0^{o}$) respectively after 24 hours, with corresponding recovery rates of 83.01 %/h, 173.58 %/h and 426.42 %/h, respectively. The steps seen in the recovery ratio curves (as well as other angle recovery ratio curves presented further in this chapter) at around one hour were due to the raise of the environmental temperature by 3-5^{o}C once a more heavily insulated lid (i.e. the original lid of the circulating bath) replaced the transparent PMMA panel upon completion of the first one hour of automatically taking images of the samples.

The test attempted to assess the recovery under more applicable thermo-mechanical conditions resembling a thermoforming process than current literature methods by inducing out-of-plane deformation rather than uniaxial stretching. The substrates never showed any observable recover in our tests, for any environmental temperature condition, indicating that all recovery observed was attributed to the films. During the recovery process at environmental temperatures higher than each TPU's T_g (around 20^{o}C), each stretched film started to recover to its original dimension. To some

extent, the recovery behavior of our formed laminates was analogous to studies in the literature combining pre-elongated TPU sheets with non-elongated elastic polymer sheets (Chen et al., 2010a, Chen et al., 2008). Therefore, the higher the Young's modulus of the TPU layer, the more dominant will be its recovery stresses over the substrate and thus higher angle recovery ratios and recovery rates for the laminates were achieved.

The results from the model confirmed the reason stated above. As shown in **Figure 6-2** below, the recovery stress applied to the PP layer by a stretched TPU increased with the Young's modulus of that film from low to high. During the first 5 min of recovery, TPU layers experienced two processes simultaneously that would significantly affect their recovery stresses - heating process and relaxation. During the recovery test, the temperature of the laminate increased rapidly from below T_g to 45^{o}C, which transitioned the TPU film from its frozen formed state to a state of higher mobility where its recovery behaviour was exhibited; during that same rapid heating period the Young's modulus of both film and substrate decreased, and their relaxation rate increased, both which lowered the output recovery stresses in the laminate. The peaks in the curves shown in **Figure 6-2** represented the maximum recovery stress values that were transferred to the PP layer from the TPU layer. Furthermore, higher relaxation time of the TPU layer contributes to a higher recovery rate for the laminate in the first 5 minutes of recovery. As shown in **Figure 6-3**, with the increase in relaxation time of TPU-High at its T_g (λ_{1g}), a higher angle recovery ratio was achieved in the first 5 minutes based on the model. This phenomenon arises because higher relaxation time mean a slower decline in

elastic modulus occurred over that initial 5 minute period, which translates to higher retention of recovery stresses for the laminate.

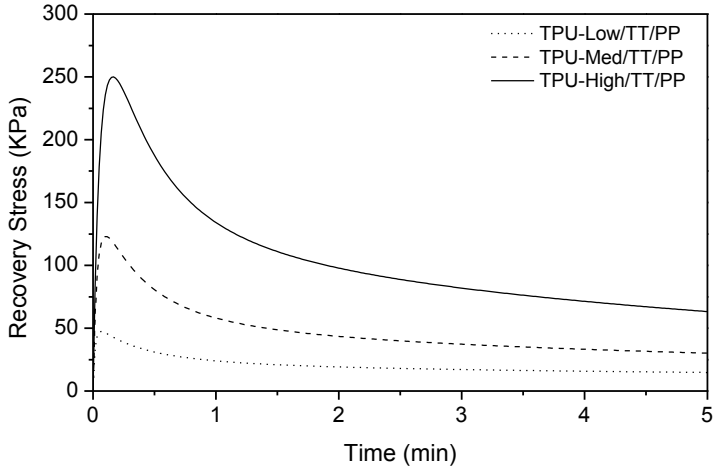

Figure 6-2 Recovery stress applied on PP layer by stretched TPU based on the model during the recovery process in the first 5 minutes at an environmental temperature of 45°C

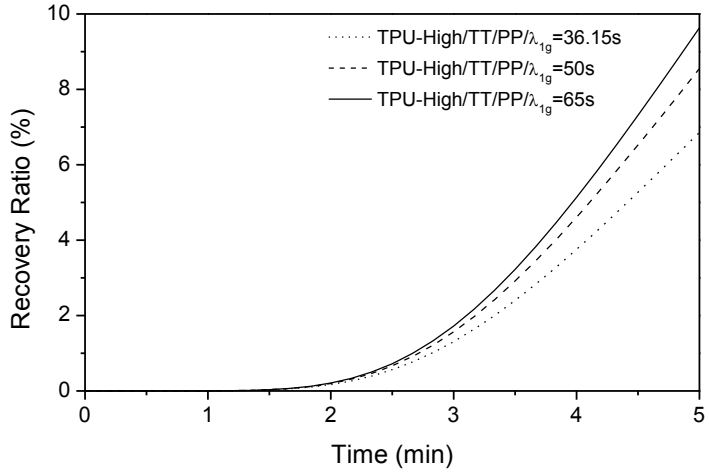

Figure 6-3 Angle recovery ratio curves of PP based laminates with TPU-High at an environmental temperature of 45°C with an increasing relaxation time of TPU-High at its T_g (λ_{1g}, calculated based on the model)

6.2 Influence of Substrates' Properties on Recovery Behaviour of Laminate

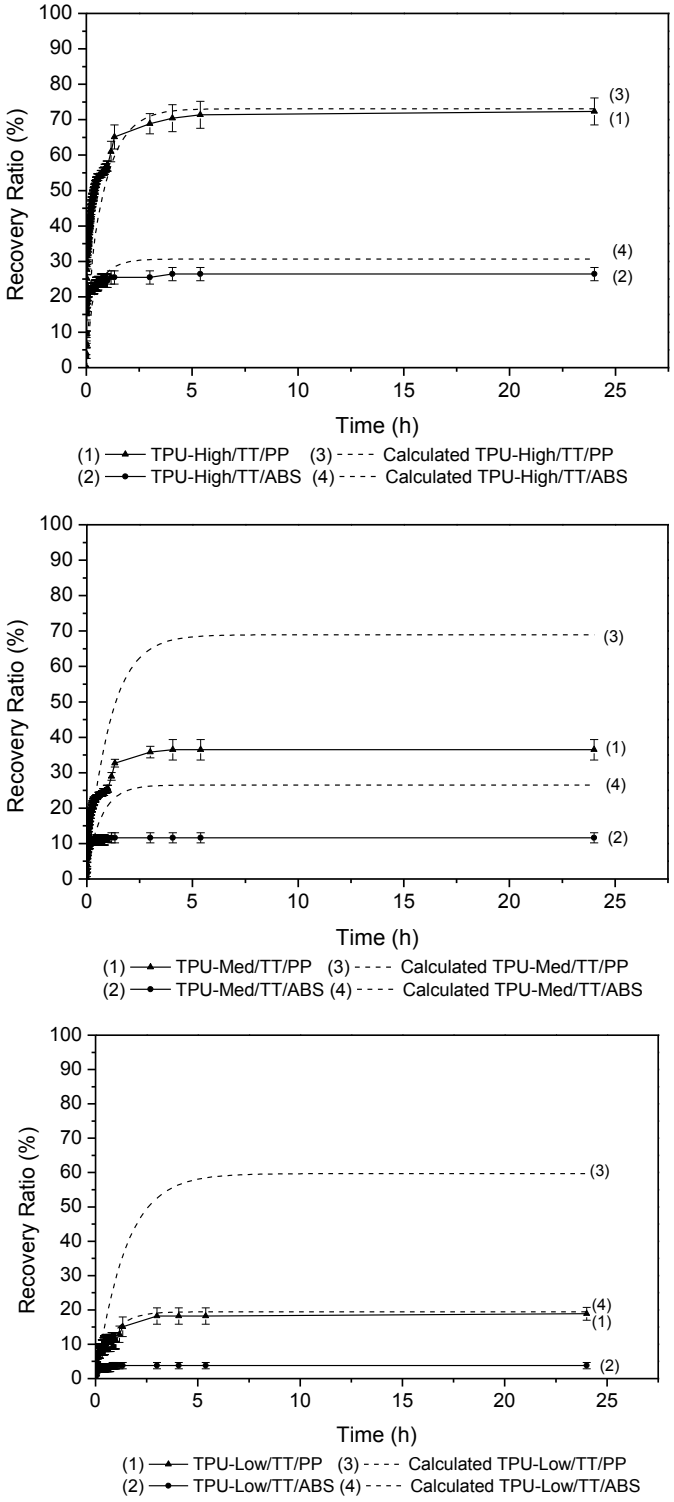

Figure 6-4 Angle recovery ratio curves (form both experiment and model) of laminates with different TPU films/ 3M tape transfer adhesive/ different substrates at an environmental temperature of 45^{o}C

Table 6-2 Final angle recovery ratios after 24h ($R_{a,\,final}$, %) and recovery rates (%/h) of laminates with different TPU films/ 3M tape transfer adhesive/ ABS at an environmental temperature of 45°C

Laminates	Final angle recovery ratio after 24h ($R_{a,\,final}$, %)	Recovery rates (%/h)	$R_{a,\,final}$ From model (%)	Recovery rates From model (%/h)
TPU-Low/TT/ABS	3.77±0.94	33.96	19.46	11.54
TPU-Med/TT/ABS	11.64±1.44	109.43	26.54	24.42
TPU-High/TT/ABS	26.42±1.89	245.28	30.67	52.27

The angle recovery ratio curves with ABS based laminates shown in **Figure 6-4** and final angle recovery ratios and recovery rates shown in **Table 6-2** further confirmed the impact that the TPU with different modulus had on recovery behaviour of laminates. As we can see, the difference in substrate layers also played an important role during the recovery process. Substituting PP with ABS obviously lowered the angle recovery ratio and recovery rate. The final angle recovery ratio of formed ABS based laminates using the same transfer tape adhesive with TPU films of Young's modulus from low to high were 3.77±0.94% (102°±1.0°), 11.64±1.44% (94°±1.5°) and 26.42±1.89% (78°±2.0°), respectively after 24 hours and the corresponding recovery rates were 33.96 %/h, 109.43 %/h and 245.28 %/h respectively as shown in **Table 6-2**, which were lower than those of corresponding PP based laminates in **Table 6-1**. The angle recovery ratios of all three ABS based laminates were stable in the first 30 minutes.

During the recovery process, the recovery stresses generated by the TPU were transferred into the substrate layer, producing a restorative bending moment in the direction of recovery (solid line in **Figure 6-5** below) which will be balanced against the

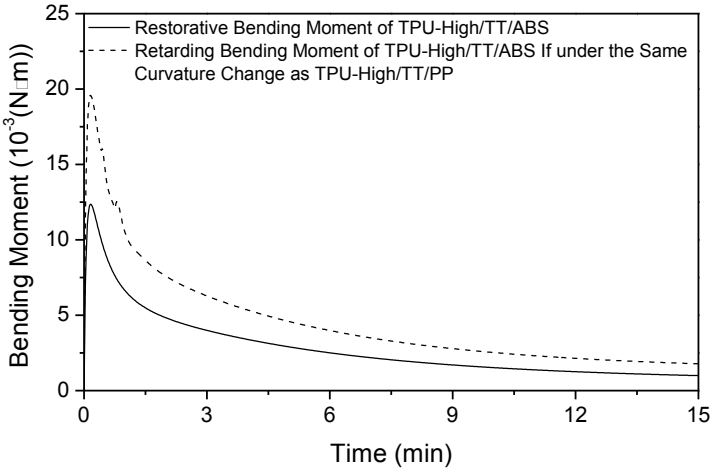

Figure 6-5 Bending moments for the recovery of TPU-High based laminates in the first 15 minutes at an environmental temperature of 45°C (calculated based on the model)

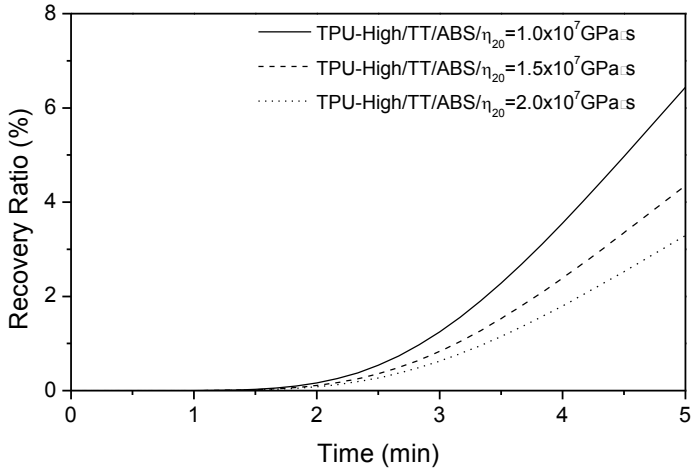

Figure 6-6 Angle recovery ratio curves of TPU-High based laminates with an increasing viscosity of ABS (η_{20}) at an environmental temperature of 45°C (calculated based on the model with keeping the Young's modulus of ABS same)

retarding bending moment produced by the substrate layer due to its corresponding curvature. During the recovery process, the imbalance of the above mentioned two bending moments were the major driving force for the recovery behaviour in the formed laminates. Thus, a substrate with larger Young's modulus should be expected to generate a larger retarding bending moment under the same curvature. The explanation above is well supported by the model results as shown in **Figure 6-5**. Assuming the ABS based laminate with TPU-High went through the same curvature changes as the PP based laminate with the same film at 45^{o}C, the ABS layer should generate a lager retarding bending moment (dashed line in **Figure 6-5**). The increased resistance to deform by ABS during recovery should reduce the angle recovery ratio as well as slow down the recovery rate of its formed laminates. The peaks in bending moments shown in **Figure 6-5** were a result of influences by both curvature change for the formed laminate (increasing the retarding bending moment) and relaxation (decreasing the retarding bending moment) during the recovery process. For similar substrate layers of identical Young's moduli, higher relaxation time of substrate (i.e. higher viscosity, η_{20}) will slow the decline in elastic modulus in the first 5 minutes of recovery (as discussed in Section 6.1) thus decreasing the recovery rate, as shown in **Figure 6-6** above.

6.3 Influence of Recovery Temperature on Recovery Behaviour of Laminate

The influence of environmental temperature on the recovery behaviour of laminates is mainly due to temperature-dependent properties such as Young's modulus and relaxation time of both TPU and substrate layers. The experimental angle recovery ratio curves shown in the **Figure 6-7** (PP based laminates) and **Figure 6-8** (ABS based

laminates) depicted the trend that at higher environmental temperature (now 65^{o}C rather than 45^{o}C) led to a higher angle recovery ratio and recovery rate, particularly for laminates with the TPU-Low and TPU-Med films. It seemed that the laminates with TPU-Low and TPU-Med films were more sensitive to temperature. As shown in **Table 6-3**, the final angle recovery ratios for the formed PP based laminates with TPU films of Young's modulus from low to high were 62.58%±2.37% (39.7^{o}±2.5^{o}), 69.81%±2.83% (32.0^{o}±3.0^{o}) and 83.02%±3.77% (18.0^{o}±4.0^{o}), respectively at 65^{o}C after 24 hours and the recovery rates were 271.70 h^{-1}, 328.30 h^{-1} and 354.72 h^{-1} respectively, which were higher than those of the corresponding PP based laminates at 45^{o}C shown in **Table 6-1** (except for the laminate with TPU-High which is due to the anomalistic decrease of relaxation time of TPU-High films from 45 ^{o}C to 65^{o}C as shown earlier in **Figure 4-11**). In terms of the ABS based laminates, the final angle recovery ratios with TPU films of Young's modulus from low to high were 10.38%±1.33% (95.0^{o}±1.4^{o}), 26.42%±2.67% (88.0^{o}±2.8^{o}) and 34.91%±1.33% (69.0^{o}±1.4^{o}), respectively at 65^{o}C after 24 hours and the recovery rates were 39.62 %/h, 169.80 %/h and 311.32 %/h respectively, which are higher than those of corresponding ABS based laminates at 45^{o}C. The angle recovery ratio curves of PP based laminates showed a continuing increasing trend at 65^{o}C, not the plateau seen for PP based laminates at 45^{o}C nor for ABS based laminates at 65^{o}C, as seen by the data after 25 hours.

The reason for the differences in angle recovery ratio seen at this higher temperature cannot be explained only by considering the temperature-dependent property of Young's moduli among the material components of these laminates, but also needed to

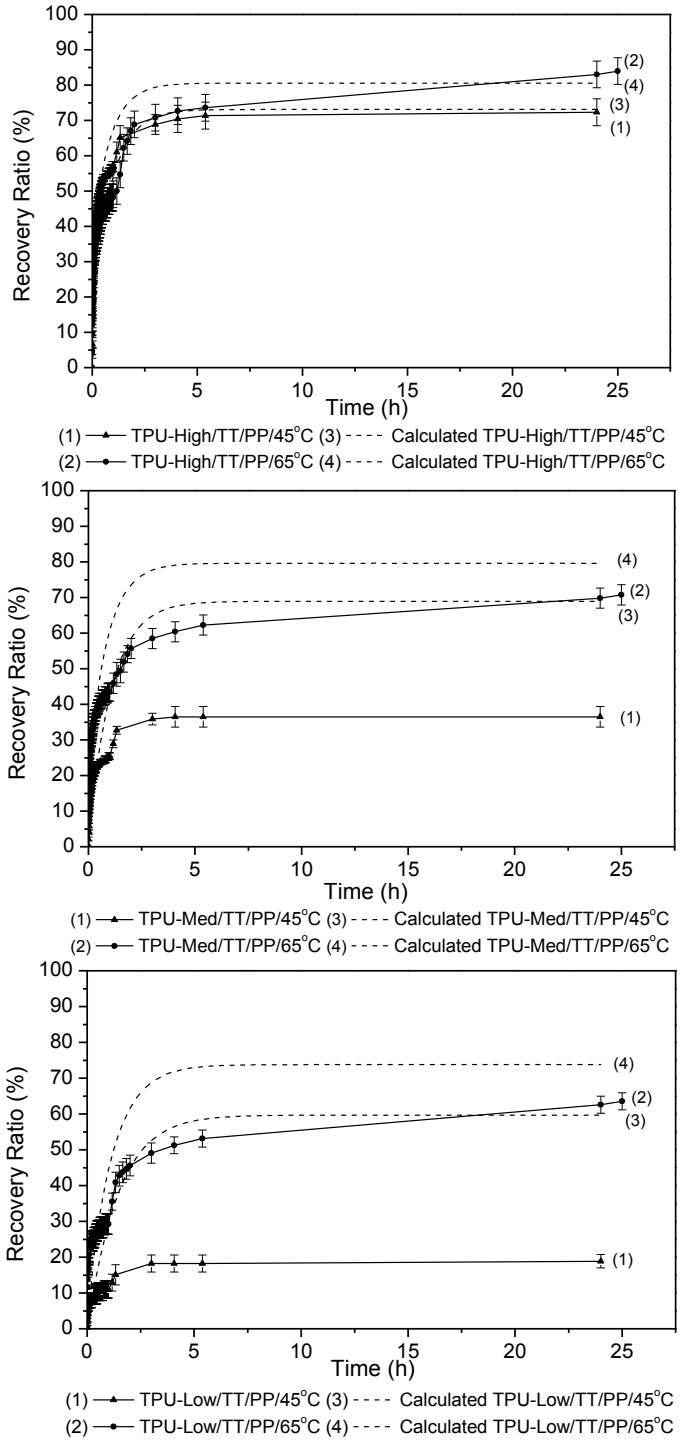

Figure 6-7 Recovery ratio curves of laminates with different TPU films/ 3M tape transfer adhesive/ PP at different environmental temperature of 45°C and 65°C. Laminates with any TPU at 15 °C never showed any observable recover in our tests, and their values of recovery ratio from the model were negligible, so the curves at 15°C were not shown in the Figure. Same with ABS based laminates

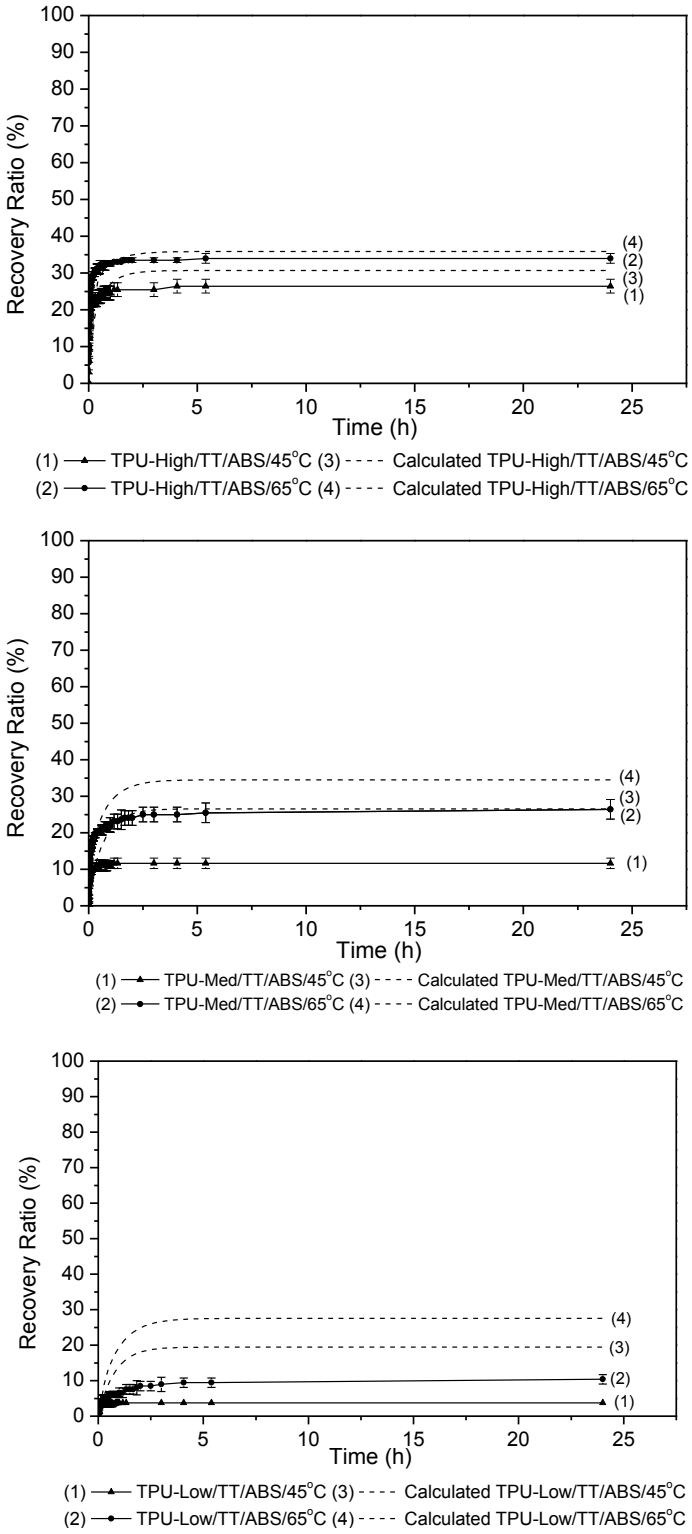

Figure 6-8 Recovery ratio curves of laminates with different TPU films/ 3M tape transfer adhesive/ ABS at different environmental temperature of 45°C and 65°C

Table 6-3 Final angle recovery ratio after 24h ($R_{a,\,final}$, %) and recovery rates (%/h) of laminates with different TPU films/ 3M tape transfer adhesive/ different substrates at different environmental temperatures of 65°C

Laminates	Final angle recovery ratio after 24h ($R_{a,\,final}$, %)	Recovery rates (%/h)	$R_{a,\,final}$ From model (%)	Recovery rates From model (%/h)
TPU-Low/TT/PP	62.58±2.37	271.70	73.78	40.74
TPU-Med/TT/PP	69.81±2.83	328.30	79.62	86.93
TPU-High/TT/PP	83.02±3.77	354.72	80.57	140.11
TPU-Low/TT/ABS	10.38±1.33	39.62	27.56	20.67
TPU-Med/TT/ABS	26.42±2.67	169.80	34.51	44.40
TPU-High/TT/ABS	34.91±1.33	311.32	35.85	72.15

consider their time-dependent property. It is the relaxation modulus among the material components of these laminates that are contributing to the balance of the two opposite bending moments at the later period of the recovery process. As shown earlier in **Figure 4-12** and **Figure 4-13** with the increase of environmental temperature from 45°C to 65°C, there was a drop in the relaxation modulus for the TPU, stated from low to high as 1.83%, 3.31% and 9.43%, while for the PP and ABS the drop in relaxation modulus was 34.26% and 47.85%, respectively. Therefore, the stress state of the TPU layer became increasingly dominant over the PP or ABS layer as time progressed at the higher temperature of 65°C, which pushed the laminates to a higher extent of recovery.

6.4 Influence of Draw on Recovery Behaviour of Laminate

The angle recovery ratio results with the PP based laminates for different draw values (DV) at an environmental temperature of 45^{o}C are shown in **Figure 6-9** and **Table 6-4**. The maximum out-of-plane draw for the PP based laminates with TPU films of low, medium and high Young's modulus was 10mm, 11mm and 12mm, respectively, and beyond that limit in each case the film layer of the laminate would fail during forming. The effect of larger pre-strain on the recovery behaviour of the TPU based laminates was hypothesized to produce higher recovery stresses directed towards the substrate during the recovery stage, thus expectedly increasing the angle recovery ratio and recovery rate, which is shown in the calculated curves in **Figure 6-9** based on the model. From the experimental results, for the differing extent of draw from 6 mm to 10mm, the angle recovery ratios and recovery rates of PP based laminates increased with differing TPU films (a slight decrease happened for laminates using TPU-Med). However, this trend was inversed when the draw was increased beyond 10mm (only seen for the laminates with TPU-Med and TPU-High as TPU-Low broke beyond 10mm). With the further draw, both angle recovery ratio and recovery rate decreased. For TPU-Med based laminates, the final angle recovery ratio for draw of 10mm versus 11mm was 36.48%± 2.89% (67^{o}±3.1^{o}) versus 24.08%± 6.38% (85.0^{o}±7.1^{o}) respectively at 45 ^{o}C after 24 hours and the recovery rates were 173.58 %/h and 74.53 %/h, respectively. The same trend in final angle recovery ratio was seen in more detail with the TPU-High based laminates since it could be drawn to 12 mm into the mold cavity. For draw values of 10mm, 11mm and 12mm, the final angle recovery ratio was 72.33%± 3.81% (29^{o}±4.0^{o}), 51.74%± 1.79% (54.0^{o}±2.0^{o}) and 46.86%± 5.55% (62.3^{o}±6.5^{o}) respectively at 45 ^{o}C after 24 hours and the

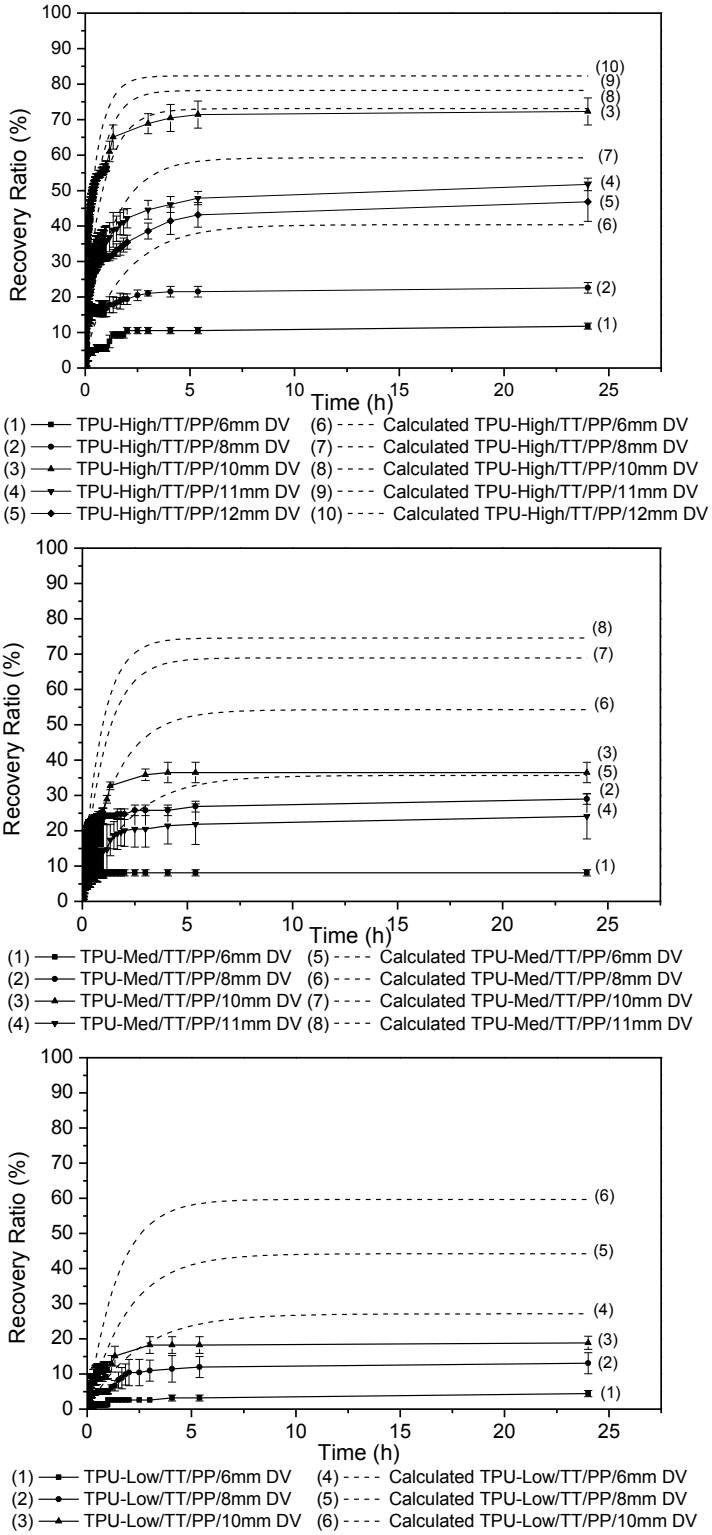

Figure 6-9 Recovery ratio curves of laminates with different TPU films/ 3M tape transfer adhesive/ PP with different draw values (DV)at environmental temperature of 45^{o}C

Table 6-4 Final angle recovery ratio after 24h ($R_{a,\,final}$, %) and recovery rates (%/h) of laminates with different TPU films/ 3M tape transfer adhesive/ PP with different draw values (DV) at environmental temperature of 45°C

Laminates	Final angle recovery ratio after 24h ($R_{a,\,final}$, %)	Recovery rates (%/h)	$R_{a,\,final}$ From model (%)	Recovery rates From model (%/h)
TPU-Low/TT/PP/6mmDV	4.40 ± 0.87	8.4	27.12	5.15
TPU-Low/TT/PP/8mmDV	13.05± 3.00	29.4	44.21	10.39
TPU-Low/TT/PP/10mmDV	18.87±1.89	83.0	59.69	18.30
TPU-Med/TT/PP/6mmDV	8.10 ± 0.87	89.85	35.66	10.91
TPU-Med/TT/PP/8mmDV	28.96 ± 1.50	175.72	54.26	21.99
TPU-Med/TT/PP/10mmDV	36.48± 2.89	173.58	68.94	38.63
TPU-Med/TT/PP/11mmDV	24.08 ± 6.38	74.53	74.55	49.42
TPU-High/TT/PP/6mmDV	11.80 ± 0.87	45.4	40.37	23.44
TPU-High/TT/PP/8mmDV	22.60 ± 1.50	143.9	59.22	47.08
TPU-High/TT/PP/10mmDV	72.33 ± 3.81	426.4	73.10	82.31
TPU-High/TT/PP/11mmDV	51.74 ± 1.79	242.0	78.22	104.99
TPU-High/TT/PP/12mmDV	46.86 ± 5.55	214.5	82.33	131.46

recovery rates were 426.4 %/h, 242.0 %/h and 214.5 %/h respectively. The reason why a higher draw value beyond 10mm leads to a lower angle recovery ratio and recovery rate still needs further investigated but could be related to creep.

6-5 Analysis on Discrepancy of Final Angle Recovery Ratio between Model and Experimental Results

The final angle recovery ratio ($R_{a,\,final}$, %) was treated as the critical indicator from our experiments for classifying the recovery nature of TPU based laminates. As seen in the figure within above sections, results from the model gave similar trends as obtained from experiments with respect to the variables of study (namely film modulus, substrate type, environmental temperatures and extent of draw) in regards to the $R_{a,\,final}$. However, the magnitude of model $R_{a,\,final}$ rarely matched experimental results; mostly the model values were higher than those from experiments, in reference to **Table 6-1** to **Table 6-4**. The model suggests that $R_{a,\,final}$ is mainly dependant on the moduli of TPU and substrates layers as well as the stress transfer ratio through the adhesive layer (*TR*). Since the values of modulus of both TPU and substrates in model were obtained from fitted experimental data, the choice was to treat *TR* as an adjustable parameter. The previous model results presented in Sections 6.1-6.4 were obtained based on the assumption that the value of *TR* was a constant of 3% under the different combinations of TPU/substrates/environmental temperatures/draw values. Best-fit *TR* values by non-linear regression to match the $R_{a,\,final}$ for different test conditions are shown in **Figure 6-10** while keeping other coefficients constant in the model.

As we can see in **Figure 6-10**, the fitted *TR* under different conditions increased with Young's modulus of the TPU films from low to high (except for the value of laminate TPU-High/TT/PP/45^{o}C/DV=8mm), which meant that less of the recovery stresses generated by the higher modulus film were dissipated during the transfer through the adhesive layer. A possible reason is better adhesion occurred at the interface between adhesive and TPU-High due to better wettability of the adhesive on their surfaces, which

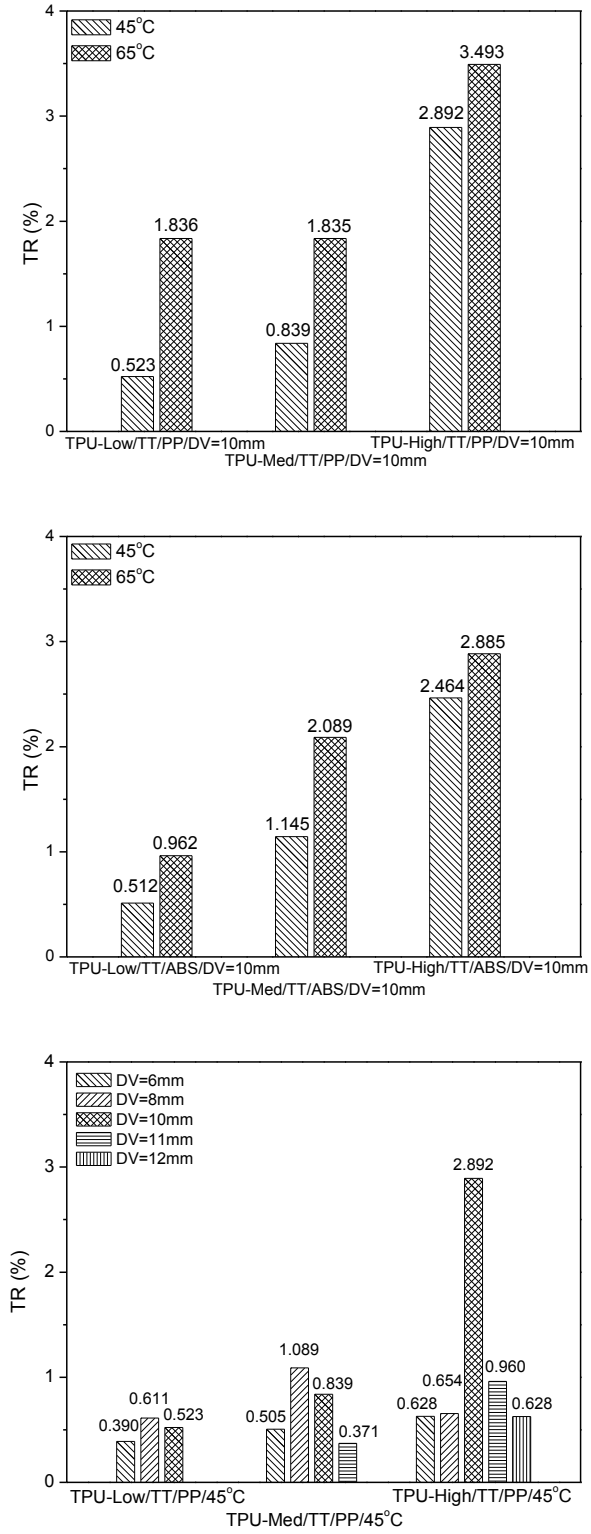

Figure 6-10 Fitted values of *TR* under different conditions based on the model

will increase the effective surface area for adhesion per unit area (Good, 1992). To examine this point, wettability of a surface in this discussion will be characterized by its water contact angle, made between a water droplet and surface (Jung and Bhushan, 2006). Water contact angles values on surfaces of the TPU films and substrates (measured by a Drop Shape Analysis System DSA10, KRÜSS GmbH, analyzed by software DSA, KRÜSS GmbH (registered version)) are shown in **Figure 6-11**. As seen from the measurement, the water contact angle decreases with increasing Young's modulus of the TPU films. In terms of adhesion, the smaller contact angles indicated that the solid surfaces were more hydrophilic and thus more compatible with the adhesive. Thus, better wetting seems to be a reasonable explanation for the trend in *TR*. This explanation also seems to apply to the differences seen between the two substrates, with the PP based laminates having a higher *TR* versus the ABS based laminates. Since wettability explained the discrepancies seen between model and experimental data well, it was felt unnecessary to entertain alternative explanations.

The fitted values of *TR* were found to increase with the environmental temperature from 45^{o}C to 65^{o}C, which indicated better adhesion at a higher environmental temperature. Besides, it was also showed that *TR* values of TPU-Low and TPU-Med based laminates decreased more rapidly with the environmental temperature from 45^{o}C to 65^{o}C, which explained the phenomenon in Section 6-3 that laminates with TPU-Low and TPU-Med films were more sensitive to temperature. It seems a better wettability of adhesive on the surface of TPU films was achieved by increasing

environmental temperature due to a more significant viscosity property of adhesive at a higher temperature (Prasath Balamurugan et al., 2013).

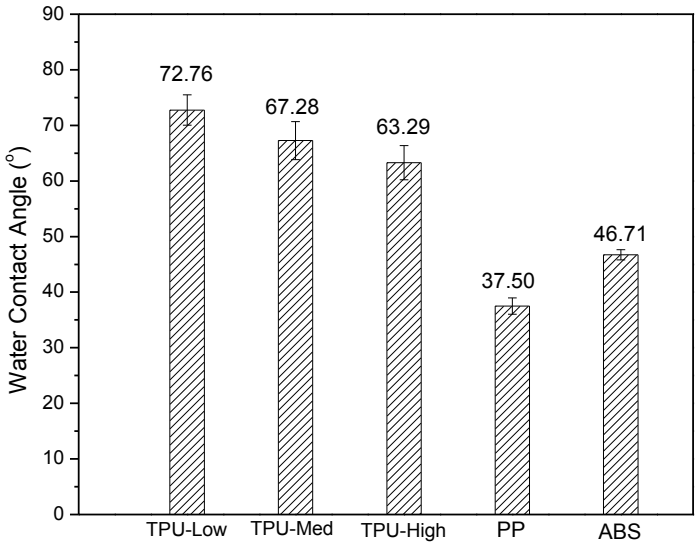

Figure 6-11 Water contact angle of TPU films and substrates at room temperature

In terms of the effect from draw, a maxima for *TR* was found, with the highest fitted values of *TR* occurring at draw values between 8-10mm. A possible failure in adhesion may be the reason for this trend but needs to be verified by further investigation.

Chapter 7 Conclusion

In this thesis, TPU and substrate properties were characterized by an easy-to-control thermoforming method, and a precise recovery measurement method was designed and implemented. In order to quantify and analyze the shape memory behavior of TPU based laminates after thermoforming, the influences of different TPU films (TPU-Low, TPU-Med and TPU-High with different modulus), different substrates (PP and ABS), different environmental temperatures (15^{o}C, 45^{o}C and 65^{o}C) as well as varied extents of deep draw (i.e. 6, 8, 10, 11 and 12mm) were examined for their influence on the recovery behaviour. This recovery was quantified experimentally and analyzed by an analytical model. All TPU films examined in this project had a T_g at 19-25℃ based on DSC tests and exhibited a dramatic change in Young's modulus and relaxation time when the temperature rose across their $T_{g.}$

Main findings were as follows:

1. The final angle recovery ratio and recovery rate of deformed laminated based on the class of TPU shape memory polymer supplied by 3M Canada increased with the modulus of the TPU film from low to high. Higher relaxation time for the TPU layer yielded a higher recovery rate for the laminate during the first five minutes of recovery;

2. Substrates of higher modulus (ABS) lowered the final angle recovery ratio and recovery rate achievable for a formed laminate. A higher relaxation time of the substrates resulted in a lower recovery rate for the laminate in the first 5 minutes of recovery;

3. The influence of ambient temperature on the recovery behaviour of laminates was mainly due to temperature-dependent and time-dependent properties such as Young's modulus and relaxation time of both TPU and substrate layers. Increasing the ambient temperature increased both the final angle recovery ratios and recovery rates of formed TPU based laminates;

4. As to the differing extent of draw from 6 mm to 10mm, the final angle recovery ratios and recovery rates of formed laminates increased for all TPU films but this trend was reversed when the draw was increased beyond 10mm.

References

Allard, R., Charrier, J. M., Ghosh, A., Marangou, M., Ryan, M. E., Shrivastava, S. & Wu, R. 1986. An Engineering Study of the Thermoforming Process: Experimental and Theoretical Considerations. *Journal of Polymer Engineering.*

Beer, F. P., Johnston, E. R., Dewolf, J. T. & Mazurek, D. F. 2009. *Mechanics of Materials,* New York, McGraw-Hill.

Behl, M. & Lendlein, A. 2007. Shape-memory polymers. *Materials Today,* 10**,** 20-28.

Behl, M., Razzaq, M. Y. & Lendlein, A. 2010. Multifunctional Shape-Memory Polymers. *Advanced Materials,* 22**,** 3388-3410.

Chen, S., Hu, J., Liu, Y., Liem, H., Zhu, Y. & Meng, Q. 2007. Effect of molecular weight on shape memory behavior in polyurethane films. *Polymer International,* 56**,** 1128-1134.

Chen, S., Hu, J. & Zhuo, H. 2010a. Properties and mechanism of two-way shape memory polyurethane composites. *Composites Science and Technology,* 70**,** 1437-1443.

Chen, S., Hu, J., Zhuo, H. & Zhu, Y. 2008. Two-way shape memory effect in polymer laminates. *Materials Letters,* 62**,** 4088-4090.

Chen, S.-C., Li, H.-M., Huang, S.-T. & Wang, Y.-C. 2010b. Effect of decoration film on mold surface temperature during in-mold decoration injection molding process. *International Communications in Heat and Mass Transfer,* 37**,** 501-505.

Chen, W. & Schlick, S. 1990. Study of phase separation in polyurethanes using paramagnetic labels: effect of soft-segment molecular weight and temperature. *Polymer,* 31**,** 308-314.

Chen, Y.-C. & Lagoudas, D. C. 2008a. A constitutive theory for shape memory polymers. Part I: Large deformations. *Journal of the Mechanics and Physics of Solids,* 56**,** 1752-1765.

Chen, Y.-C. & Lagoudas, D. C. 2008b. A constitutive theory for shape memory polymers. Part II: A linearized model for small deformations. *Journal of the Mechanics and Physics of Solids,* 56**,** 1766-1778.

Choi, N.-y. & Lendlein, A. 2007. Degradable shape-memory polymer networks from oligo[(l-lactide)-ran-glycolide]dimethacrylates. *Soft Matter,* 3**,** 901-909.

Chun, B. C., Cho, T. K. & Chung, Y. C. 2007. Blocking of soft segments with different chain lengths and its impact on the shape memory property of polyurethane copolymer. *Journal of Applied Polymer Science,* 103**,** 1435-1441.

del Río, E., Lligadas, G., Ronda, J. C., Galià, M., Cádiz, V. & Meier, M. A. R. 2011. Shape Memory Polyurethanes from Renewable Polyols Obtained by ATMET Polymerization of Glyceryl Triundec-10-enoate and 10-Undecenol. *Macromolecular Chemistry and Physics,* 212**,** 1392-1399.

Fried, J. 2003. *Polymer Science and Technology,* Pearson Education.

Gall, K., Yakacki, C. M., Liu, Y., Shandas, R., Willett, N. & Anseth, K. S. 2005. Thermomechanics of the shape memory effect in polymers for biomedical applications. *J Biomed Mater Res A,* 73**,** 339-48.

Ghosh, P. & Srinivasa, A. R. 2013. A two-network thermomechanical model and parametric study of the response of shape memory polymers. *Mechanics of Materials,* 60**,** 1-17.

Good, R. J. 1992. Contact angle, wetting, and adhesion: a critical review. *Journal of Adhesion Science and Technology*, 6**,** 1269-1302.

Jeong, H., Lee, S. & Kim, B. 2000. Shape memory polyurethane containing amorphous reversible phase. *Journal of Materials Science,* 35**,** 1579-1583.

Ji, F. L., Hu, J. L., Yu, W. M. W. & Chiu, S. S. Y. 2011. Structure and Shape Memory Properties of Polyurethane Copolymers Having Urethane Chains as Soft Segments. *Journal of Macromolecular Science, Part B,* 50**,** 2290-2306.

Jung, Y. C. & Bhushan, B. 2006. Contact angle, adhesion and friction properties of micro-and nanopatterned polymers for superhydrophobicity. *Nanotechnology,* 17**,** 4970.

Kelch, S., Steuer, S., Schmidt, A. M. & Lendlein, A. 2007. Shape-Memory Polymer Networks from Oligo[(ε-hydroxycaproate)-co-glycolate]dimethacrylates and Butyl Acrylate with Adjustable Hydrolytic Degradation Rate. *Biomacromolecules,* 8**,** 1018-1027.

Kim, B. K., Lee, S. Y., Lee, J. S., Baek, S. H., Choi, Y. J., Lee, J. O. & Xu, M. 1998. Polyurethane ionomers having shape memory effects. *Polymer,* 39**,** 2803-2808.

Koerner, H., Price, G., Pearce, N. A., Alexander, M. & Vaia, R. A. 2004. Remotely actuated polymer nanocomposites[mdash]stress-recovery of carbon-nanotube-filled thermoplastic elastomers. *Nat Mater,* 3**,** 115-120.

Krevelen, D. W. v. & Nijenhuis, K. t. 2010. *Properties of Polymers,* Singapore, Elsevier

Lan, X., Liu, Y., Lv, H., Wang, X., Leng, J. & Du, S. 2009. Fiber reinforced shape-memory polymer composite and its application in a deployable hinge. *Smart Materials and Structures,* 18**,** 024002.

Lee, S. H., Kim, J. W. & Kim, B. K. 2004. Shape memory polyurethanes having crosslinks in soft and hard segments. *Smart Materials and Structures,* 13**,** 1345.

Lendlein, A. & Kelch, S. 2002a. Shape-Memory Polymers. *Encyclopedia of Polymer Science and Technology.* John Wiley & Sons, Inc.

Lendlein, A. & Kelch, S. 2002b. Shape-Memory Polymers. *Angewandte Chemie International Edition,* 41**,** 2034-2057.

Lendlein, A., Schmidt, A. M. & Langer, R. 2001. AB-polymer networks based on oligo(ε-caprolactone) segments showing shape-memory properties. *Proceedings of the National Academy of Sciences,* 98**,** 842-847.

Leng, J. & Du, S. 2012. *Shape Memory Polymers and Multifunctional Composites,* New York, CRC Press.

Liang, C., Rogers, C. A. & Malafeew, E. 1997. Investigation of Shape Memory Polymers and Their Hybrid Composites. *Journal of Intelligent Material Systems and Structures,* 8**,** 380-386.

Lin, J. R. & Chen, L. W. 1998a. Study on shape-memory behavior of polyether-based polyurethanes. I. Influence of the hard-segment content. *Journal of Applied Polymer Science,* 69**,** 1563-1574.

Lin, J. R. & Chen, L. W. 1998b. Study on shape-memory behavior of polyether-based polyurethanes. II. Influence of soft-segment molecular weight. *Journal of Applied Polymer Science,* 69**,** 1575-1586.

Liu, Y., Gall, K., Dunn, M. L., Greenberg, A. R. & Diani, J. 2006. Thermomechanics of shape memory polymers: Uniaxial experiments and constitutive modeling. *International Journal of Plasticity,* 22**,** 279-313.

Liu, Y., Gall, K., Dunn, M. L. & McCluskey, P. 2003. Thermomechanical recovery couplings of shape memory polymers in flexure. *Smart Materials and Structures,* 12**,** 947.

Madbouly, S. A. & Lendlein, A. 2010. Shape-Memory Polymer Composites. *Shape-Memory Polymers.* Berlin: Springer Berlin Heidelberg.

Madbouly, S. A., Otaigbe, J. U., Nanda, A. K. & Wicks, D. A. 2007. Rheological Behavior of POSS/Polyurethane−Urea Nanocomposite Films Prepared by Homogeneous Solution Polymerization in Aqueous Dispersions. *Macromolecules,* 40**,** 4982-4991.

Meng, Q., Hu, J., Liu, B. & Zhu, Y. 2009. A Low-Temperature Thermoplastic Anti-bacterial Medical Orthotic Material Made of Shape Memory Polyurethane Ionomer: Influence of Ionic Group. *Journal of Biomaterials Science, Polymer Edition,* 20**,** 199-218.

Nguyen, T. D., Jerry Qi, H., Castro, F. & Long, K. N. 2008. A thermoviscoelastic model for amorphous shape memory polymers: Incorporating structural and stress relaxation. *Journal of the Mechanics and Physics of Solids,* 56**,** 2792-2814.

Oprea, S. 2009. Effect of Composition and Hard-segment Content on Thermo-mechanical Properties of Cross-linked Polyurethane Copolymers. *High Performance Polymers,* 21**,** 353-370.

Overney, R. M., Buenviaje, C., Luginbühl, R. & Dinelli, F. 2000. Glass and Structural Transitions Measured at Polymer Surfaces on the Nanoscale. *Journal of Thermal Analysis and Calorimetry,* 59**,** 205-225.

Prasath Balamurugan, G., Pukadyil, R. N., Nielsen, K. E., Brandys, F. A. & Thompson, M. R. 2013. Role of a micro-patterned adhesive interface on the performance of thermoformable multi-layered decorative polymeric film laminates. *International Journal Of Adhesion and Adhesives,* 44**,** 78-90.

Qi, H. J., Nguyen, T. D., Castro, F., Yakacki, C. M. & Shandas, R. 2008. Finite deformation thermo-mechanical behavior of thermally induced shape memory polymers. *Journal of the Mechanics and Physics of Solids,* 56**,** 1730-1751.

Robert, L. F. & Nielsen, L. E. 1993. *Mechanical properties of polymers and composites,* CRC Press.

Rogulska, M., Kultys, A. & Pikus, S. 2008. Studies on thermoplastic polyurethanes based on new diphenylethane-derivative diols. III. The effect of molecular weight and structure of soft segment on some properties of segmented polyurethanes. *Journal of Applied Polymer Science,* 110**,** 1677-1689.

Sherman, M. & Lilli 2004. *Where the action is: Decorating with formable films,* New York, NY, ETATS-UNIS, Gardner.

Throne, J. L. 2002. Thermoforming. *Encyclopedia of Polymer Science and Technology.* John Wiley & Sons, Inc.

Throne, J. L. 2008. *Understanding thermoforming*, Hanser Verlag.

Tobushi, H., Hashimoto, T., Hayashi, S. & Yamada, E. 1997. Thermomechanical Constitutive Modeling in Shape Memory Polymer of Polyurethane Series. *Journal of Intelligent Material Systems and Structures,* 8**,** 711-718.

Tobushi, H., Okumura, K., Hayashi, S. & Ito, N. 2001. Thermomechanical constitutive model of shape memory polymer. *Mechanics of Materials,* 33**,** 545-554.

Tool, A. Q. 1946. RELATION BETWEEN INELASTIC DEFORMABILITY AND THERMAL EXPANSION OF GLASS IN ITS ANNEALING RANGE*. *Journal of the American Ceramic Society,* 29**,** 240-253.

TORAY INDUSTRIES, I. 2014. *IMF (In Mold Forming)* [Online]. Available: http://www.toray.jp/films/en/printing/process/insert.html [Accessed July 2015].

Zhang, C.-S. & Ni, Q.-Q. 2007. Bending behavior of shape memory polymer based laminates. *Composite Structures,* 78**,** 153-161.

Zhang, R., Guo, X., Liu, Y. & Leng, J. 2014. Theoretical analysis and experiments of a space deployable truss structure. *Composite Structures,* 112**,** 226-230.

Zhu, Y., Hu, J., Yeung, L.-Y., Liu, Y., Ji, F. & Yeung, K.-w. 2006. Development of shape memory polyurethane fiber with complete shape recoverability. *Smart Materials and Structures,* 15**,** 1385.

Zhu, Y., Hu, J., Yeung, L. Y., Lu, J., Meng, Q., Chen, S. & Yeung, K. w. 2007. Effect of steaming on shape memory polyurethane fibers with various hard segment contents. *Smart Materials and Structures,* 16**,** 969.

Appendices

Appendix A: MATLAB Code of Recovery Curves

Part 1: `rcurve1.m`

```
function f= rcurve1(x,y)
global R a
f= R*(pi-2*a)-(atan(y./x)-a)*(x.^2+y.^2).^(0.5)/sin(atan(y./x)-a);
end
```

Part 2: `rcurve2.m`

```
function g= rcurve2(x,y)
global R a
g= R*(pi-2*a)-(a-atan(y./x))*(x.^2+y.^2).^(0.5)/sin(a-atan(y./x));
end
```

Part 3: `recovery curve.m`

```
clear all
clc
global R h a L xc yc xd yd
R=2.5;
h=0.5;
a=asin((R-h)/R);
L=R*(pi-2*a);
xc=L*cos(a);
yc=tan(a)*xc;
xd=2*R*cos(a)*cos(2*a-pi/2);
yd=tan(2*a-pi/2)*xd;
m= ezplot(@rcurve1,[0 xc yc 6]);
set(m,'Color','blue','LineStyle','-','LineWidth',2)
hold on
n= ezplot(@rcurve2,[xc 6 yd yc]);
set(n,'Color','red','LineStyle','-','LineWidth',2)
hold on
syms x1 y1
x1=0:0.1:xc;
y1=tan(a)*x1;
plot(x1,y1,'--','Color','blue','LineWidth',2)
hold on
syms x2 y2
x2=0:0.1:xd;
y2=tan(2*a-pi/2)*x2;
plot(x2,y2,'--','Color','red','LineWidth',2)
axis([0 5 -2 5])
hold off
```

Appendix B: MATLAB Code of the Model

Part 1: `recovery.m`

```
global a0 a b c f g Tg Tw TR k hs At As e E10 Rs0 E u2 E0 u20 lambda10

T= Tg+Tw-(Tg+Tw-273)*exp(-k.*t);  % Environmental Temperature, starting
from 273K, K

% TPU properties
E1=E10*exp(a*(Tg./T-1));
lambda1=lambda10*exp((b-c)*(Tg./T-1));

% Substrate properties, for PP and ABS
E=E0*exp(f*(Tg./T-1));
u2=u20*exp(g*(Tg./T-1));
lambda2=u2./E;

dy = zeros(3,1);
dy(1)=-y(1)./lambda1+e*E1./lambda1; %y(1) is recovery stress generated
from TPU
y(3)=TR*y(1); % y(3) is transferred recovery stress
dy(2)=-y(2)./lambda2+ At*y(3)/As/(hs/(exp(hs*(1-y(2))./Rs0)-1)+hs/2-
Rs0/(1-y(2)))/u2*((hs/(exp(hs*(1-y(2))./Rs0)-1)+hs).*(a0.*(1-y(2)))-
(Rs0/(1-y(2))).*sin(a0.*(1-y(2))));
%y(2) is angle recovery ratio
end
```

Part 2: `Main Part.m`

```
clear all
clc

global h Rm a0 a b c f g Tg Tw TR k ht hs At As Rt0 L0 Lt Lts e E10 rs0
Rs0 n0 n E u2 E0 u20 lambda10 l0 ls lt deltalt deltals ht0 deltaht hs0
deltahs vs vt Ratd

%Parameter of Forming
h=0.01; % Draw values, m
Rm=25E-3; % radius of male mold, m

% Values of constant parameters in equations
Tg= 293; % TPU, K
Tw= 25; % Recovery T is Tg+Tw, K
TR=0.03;%Stress transfer ratio through the adhesive layer
k= 0.015; % Overall heat transfer coefficient of laminates, K/s
vt=0.5;% Possion's ratio of TPU
vs= 0.35;% Possion's ratio of substrate, 0.42 for PP, 0.35 for ABS
```

```
% TPU Dimension
a0= 2*acos((Rm-h)/Rm); % initial central angle after forming
hs0=0.5E-3; % original Thickness of substrate, m
Rt0=Rm+hs0; %radius of TPU, m
L0=2*(Rm^2-(Rm-h)^2)^(1/2); % initial length of laminate before forming,
m
Lt=Rt0*a0; % length of laminate after forming, m
e=(Lt-L0)/L0; % strain of TPU

l0=12.7E-3; %original width of TPU, m
deltalt=-l0*(1-(1+e)^(-vt)); % m
lt=l0+deltalt; %width of TPU after forming, m

ht0=0.2E-3; % Original thickness of TPU, m
deltaht=-ht0*(1-(1+e)^(-vt));% m
ht=ht0+deltaht; %Thickness of TPU after forming, m

At=lt*ht; % area of the cross-section of TPU, m^2

% Substrate Dimension
l0=12.7E-3; %original width of substrate, m
deltals=-l0*(1-(1+e)^(-vs));% m
ls=l0+deltals; %width of substrate after forming, m

hs0=0.5E-3; % Original Thickness of substrate, m
deltahs=-hs0*(1-(1+e)^(-vs));% m
hs=hs0+deltahs; %Thickness of substrate after forming, m

As=ls*hs; %area of the cross-section of substrate, m^2

rs0= Rm+0.5*hs; %Initial distance from center of the curve to the
centroid of substrate, m
Rs0=hs/log((rs0+0.5*hs)/(rs0-0.5*hs)); %Initial distance from center of
the curve to the N.A of substrate, m
n0=rs0-Rs0; % initial gap between Rs0 and rs0, m
Lts=Rs0*a0;% length of substrate after forming, m

% Values of coefficients of TPU films
a= 20.273; % 45C,Low, Med, High: 10.661, 15.326, 20.273
          %65C,Low, Med, High: 7.8573, 11.405, 15.518
b= 29.84; % 45C,Low, Med, High:38.26, 33.96, 29.84
         % 65C,Low, Med, High:24.5, 21.84, 17.36
c=0;
E10 =16.65E6; %45C,Low, Med, High: 4.4085E6, 9.3221E6, 16.65E6, Pa
               %65C,Low, Med, High: 4.7618, 10.383, 18.975, Pa
lambda10=36.15;%45C,Low, Med, High: 14.77, 23.17,36.15, s
              %65C,Low, Med, High: 20.225, 30.561, 48.068, s

% Values of coefficients of substrates
f=6.865; % 45C: 15.825 for PP, 6.865 for ABS
          % 65C: 15.04 for PP, 8.0325 for ABS
```

```
g=115; % 45C: 115 for PP, 115 for ABS
       % 65C: 70 for PP, 70 for ABS
E0 =941.33E6; % 45C: 360.29E6 for PP, 941.33E6 for ABS, Pa
              % 65C: 368.08E6 for PP, 911.61E6 for ABS, Pa
u20 =1.5E16;  % 45C: 1E16 for PP, 1.5E16 for ABS, Pa.s
            % 65C: 0.8E16 for PP, 1.5E16 for ABS, Pa.s

% Equations
[t,y]=ode45(@recovery,[0:1:86400],[0,0,0]);

% Environmental Temperature, Tg=293K, starting from 273K
T= Tg+Tw-(Tg+Tw-273)*exp(-k.*t);

% TPU properties
E1=E10*exp(a*(Tg./T-1)); %Young's modulus
lambda1=lambda10*exp((c-b)*(Tg./T-1)); %Relaxation time

% Substrate properties
E=E0*exp(f*(Tg./T-1));%Young's modulus
u2=u20*exp(g*(Tg./T-1));%Viscosity
lambda2=u2./E; %Relaxation time

TgT=Tg./T-1;
stress=TR*y(:,1); %Transferred recovery stress, N/m^2
F= At.*stress; % Transferred recovery force, N
at=a0*(1-y(:,2)); % Corresponding central angle at time t
Rst=Rs0./(1-y(:,2)); % Corresponding distance from center of the curve
to the N.A of substrate at time t, m
rst=hs./(exp(hs.*(1-y(:,2))./Rs0)-1)+hs/2; % Corresponding distance from
center of the curve to the centroid of substrate at time t, m
n=hs./(exp(hs.*(1-y(:,2))./Rs0)-1)+hs/2-Rs0./(1-y(:,2)); % Corresponding
gap between Rst and rst, m
Rat=100*y(:,2); % Angle recovery ratio at time t, %
Ratd=gradient(y(:,2)); % Derivative of angle recovery ratio by time t
Ms=1000*(As.*n.*E.*y(:,2)+As*n.*u2.*Ratd); % Retarding bending moment of
substrate layer at time t, 10^-3(N.m)
Mt=1000*F.*(at.*(rst+hs/2)-Rst.*sin(at)); % Restorative bending moment
on substrate layer at time t, 10^-3(N.m)

figure (1) % Environmental Temperature vs. time (t)
 plot (t/3600,T,'--')
 title('Environmental Temperature vs t')
 xlabel('t(h)');
 ylabel('T');

figure(2) % Angle recovery ratio vs. time (t)
plot(t/3600,Rat,'--')
title('Angle Recovery Ratio vs t')
xlabel('t(h)');
ylabel('Ra');

figure(3) % Transferred recovery stress vs. time (t)
```

```
plot(t/3600,stress,'--')
title('stress vs t')
xlabel('t(h)');
ylabel('stress');

figure (4) % Restorative Bending Moment vs. time (t)
 plot (t,Mt,'--')
 title('Restorative Bending Moment vs t')
 xlabel('t(s)');
 ylabel('Mt (10^-3(N.m))');

figure (5) % Retarding Bending Moment vs. time (t)
 plot (t,Ms,'--')
 title('Retarding Bending Moment vs t')
 xlabel('t(s)');
 ylabel('Ms (10^-3(N.m))');
```